

Fig. S1: Example of Feedback Vertex Set Control. (a) Network representation of the system governed by Eqs. S5-S8 and its Feedback Vertex Set Control (FC) node set. (b) Two attractors of the system governed by Eqs. S5-S8, a limit cycle (Attractor 1) and a steady state (Attractor 2). The time course of each node state variable is denoted with different line styles and colors. The colors of the FC node set match those in panel a. (c) For a target attractor of interest (left column), the control action of a node state override of the FC node set (middle column) guarantees that the system will converge to the target attractor (right column).

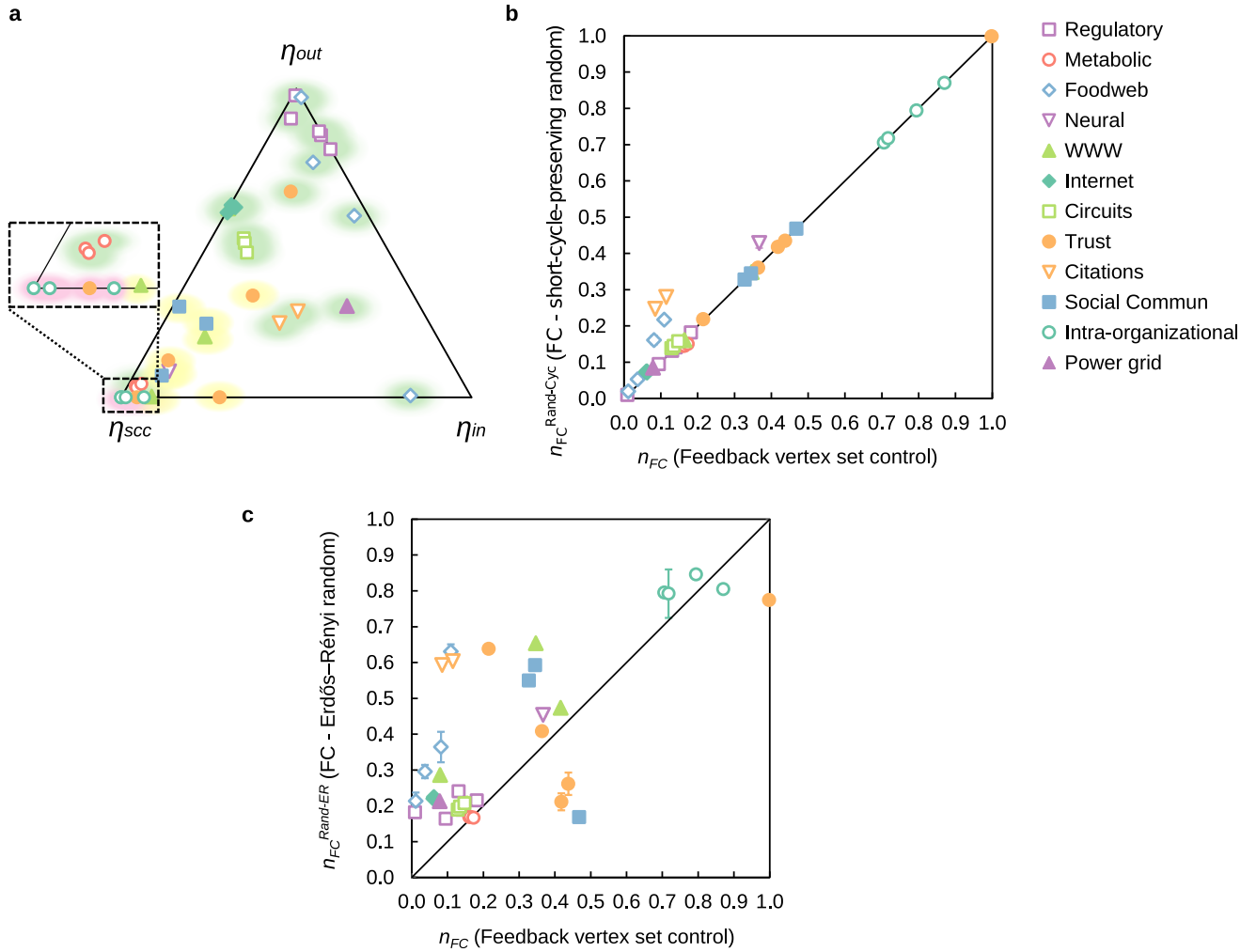


Fig. S2: Additional results on feedback vertex set control in real networks. (a) Ternary plot of the normalized fraction of nodes in an SCC ( $\eta_{SCC}$ ), in the in-component of all SCCs ( $\eta_{in}$ ), and in the out-component of all SCCs ( $\eta_{out}$ ) for each real network ( $\eta_x = N_x / (N_{SCC} + N_{in} + N_{out})$ ,  $x = SCC, in, out$ ). The position in the plot is determined by  $\eta_x$  in such a way that a point is close to the  $\eta_x$  vertex if  $\eta_x \simeq 1$  and close to the side opposite to the  $\eta_x$  vertex if  $\eta_x \simeq 0$ . Thus, networks dominated by their strongly connected component are close to the  $\eta_{SCC}$  vertex, networks dominated by their out-component are close to the  $\eta_{out}$  vertex, and networks dominated by their in-component are close to the  $\eta_{in}$  vertex. The green, yellow and pink shading is defined as in Fig. 2a. Networks with the largest FC node set size (pink shading) are dominated by their SCC, networks with an intermediate-to-high value of  $\eta_{SCC}$ , while several networks with the lowest FC node set size (green shading) are dominated by their out-component (e.g. regulatory networks) or in-component. Metabolic networks are outliers: they have one of the largest  $\eta_{SCC}$  ( $\approx 0.9$ ) yet have a small  $n_{FC}$  ( $\approx 0.25$ ) and  $n_{FVS}$  ( $\approx 0.2$ , see Fig. 2a,b). We attribute this result of metabolic networks to their low connectivity and density ( $M/N < 3$  and  $M/N^2 < 0.003$ , respectively, where  $M$  is the number of edges), which makes it easier to disrupt the cycle structure of the large SCC. (b) Scatter plot with the fraction of control nodes in FC for real networks ( $n_{FC}$ ) and their short-cycle preserving randomization ( $n_{FC}^{Rand-Cyc}$ ). (c) Scatter plot with the fraction of control nodes in feedback vertex set (FVS) control for real networks ( $n_{FC}$ , horizontal axis) and their full randomization (Erdős-Rényi,  $n_{FC}^{Rand-ER}$ ).  $n_{FC}$  in real networks shows a weak correlation with its value  $n_{FC}^{Rand-ER}$  in full randomization. The intra-organizational networks at the top-right part of the plot have a large graph density and are close to being complete graphs; because of this, the feedback vertex set of these networks and their Erdős-Rényi networks is very similar (i.e., the FVS is approximately the whole graph). Error bars denote the estimated standard deviation of the randomized ensembles.

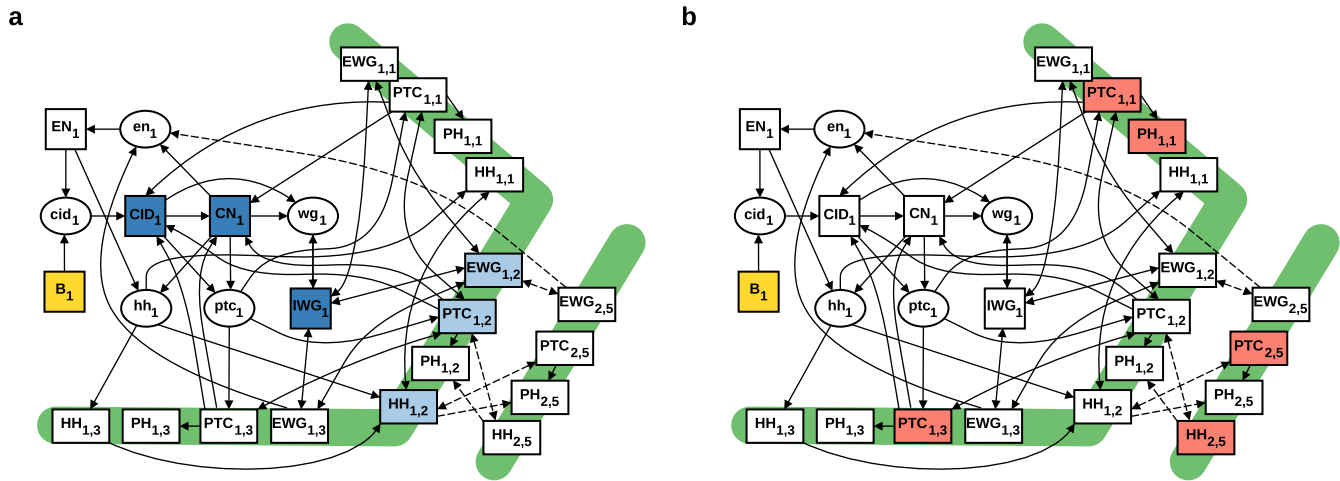


Fig. S3: Control of the von Dassow et al. model of the Drosophila segment polarity network. The figure shows a cell of the four-cell parasegment together with three of its six boundaries (green lines). The complete network contains four cells in a symmetric completion of the figure. Elliptical nodes represent mRNAs and rectangular nodes are proteins. Intracellular interactions are drawn as solid lines and intercellular interactions are dashed. Yellow nodes are source nodes. (a) Blue nodes are FC nodes in every cell. Dark blue nodes are sufficient for attractor control in the considered dynamic models. (b) Red nodes are SC nodes in every cell.

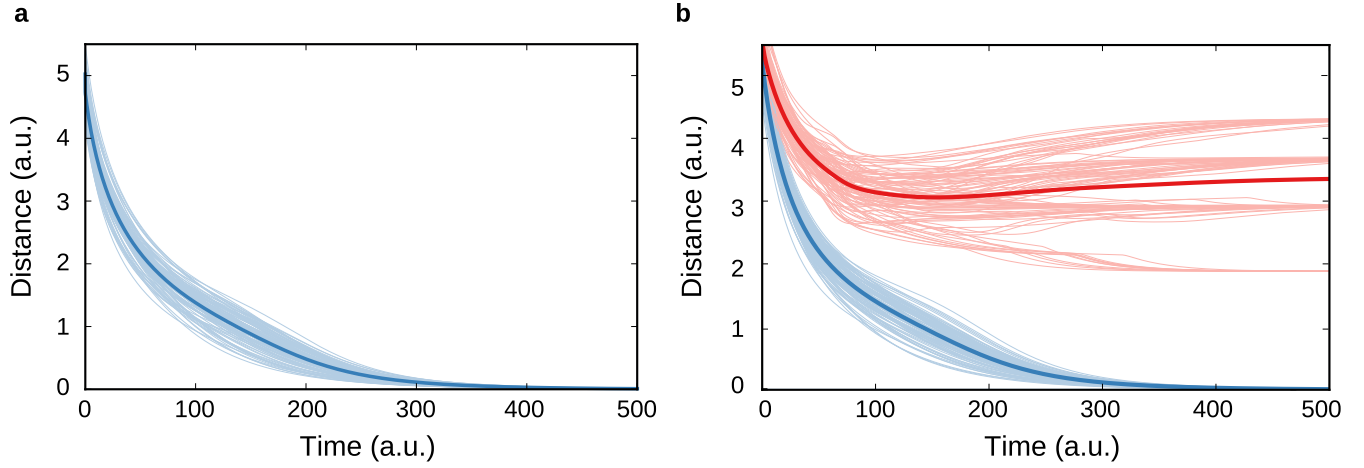


Fig. S4: Effectiveness of the control of the *Drosophila* segment polarity differential equation model. (a) The thin light blue lines indicate the evolution of the norm of the difference between the desired wild type steady state and the controlled state trajectory using FC (blue symbols on Fig. S3a) for 100 randomly chosen initial conditions. (b) The thin light blue lines are the evolution of the norm of the difference between the wild type steady state and the controlled state trajectory using reduced FC (dark blue symbols on Fig. S3a) for 100 randomly chosen initial conditions. The thin red lines indicate the norm of the difference between the uncontrolled trajectory and the wild type steady state for 100 randomly chosen initial conditions. In all initial conditions the concentration of each quantity is chosen uniformly from the interval  $[0, 1]$ . The thick blue (red) lines indicate the average of the relevant 100 realizations.

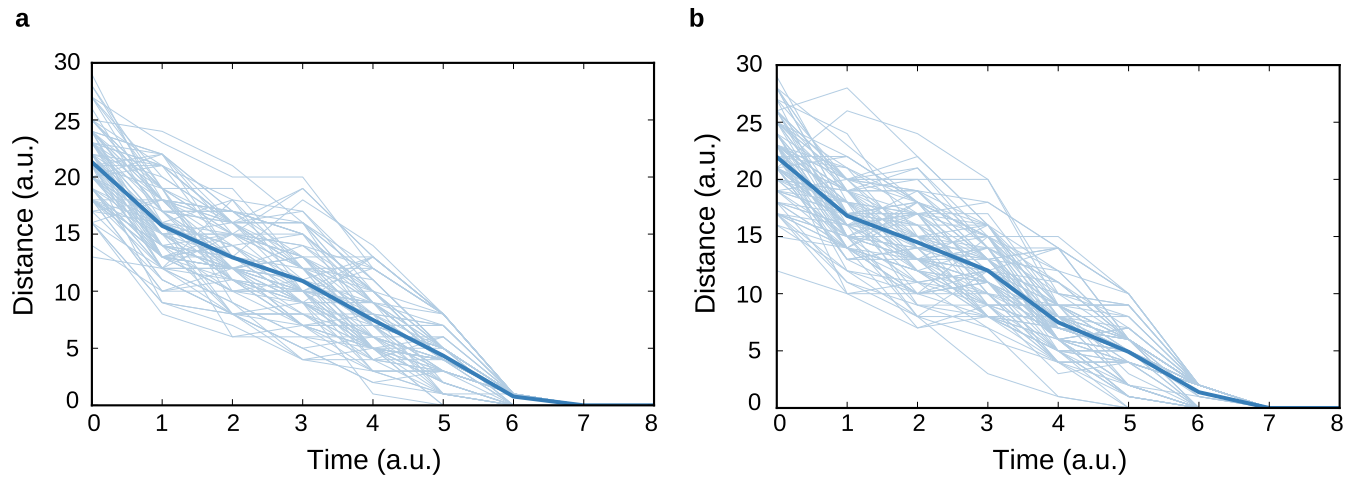


Fig. S5: Control of the Boolean model of the *Drosophila* segment polarity genes. The light blue thin lines show the evolution of the norm of the difference between the wild type steady state and the controlled state trajectory using feedback vertex set control (FC) for 100 randomly chosen initial conditions, in which the concentration of each quantity is chosen between ON and OFF with equal odds. The thick blue line is the average of the 100 realizations. (a) Control using the feedback vertex set (b) Control using the reduced feedback vertex set.

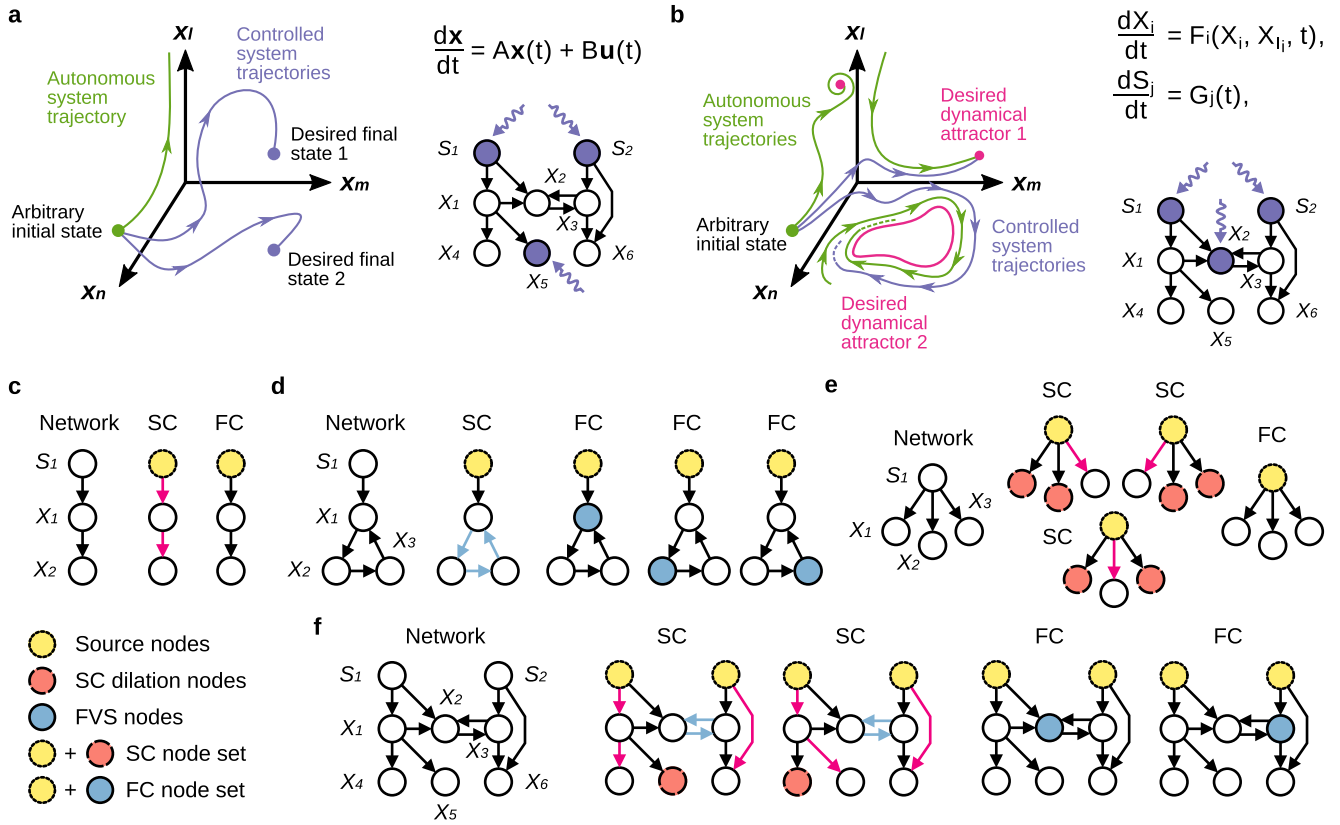


Fig. S6: Structure-based control methods. Structure-based control methods make conclusions about the dynamics of a system using solely the network structure. This figure repeats some panels from Fig. 1. (a) In structural controllability (SC) the objective is to drive the network from an arbitrary initial state to any desired final state by acting on the network with an external signal  $\mathbf{u}(t)$ . The dynamics are considered to be well-approximated by linear dynamics. (b) In feedback vertex set control (FC) the objective is to drive the network from an arbitrary initial state to any desired dynamical attractor (e.g. steady state) by overriding the state of certain nodes. (c-f) Structure-based control in simple networks. Control of the source nodes (yellow nodes with dotted outlines) is shared by SC and FC. SC additionally requires controlling certain dilation nodes (red nodes with dashed outlines) but requires no independent control of cycles. FC requires controlling all cycles by control of the feedback vertex set (FVS, blue nodes with solid outlines). The edges of the non-intersecting linear chains of nodes of SC are colored purple and the edges involved in a directed cycle are colored blue.

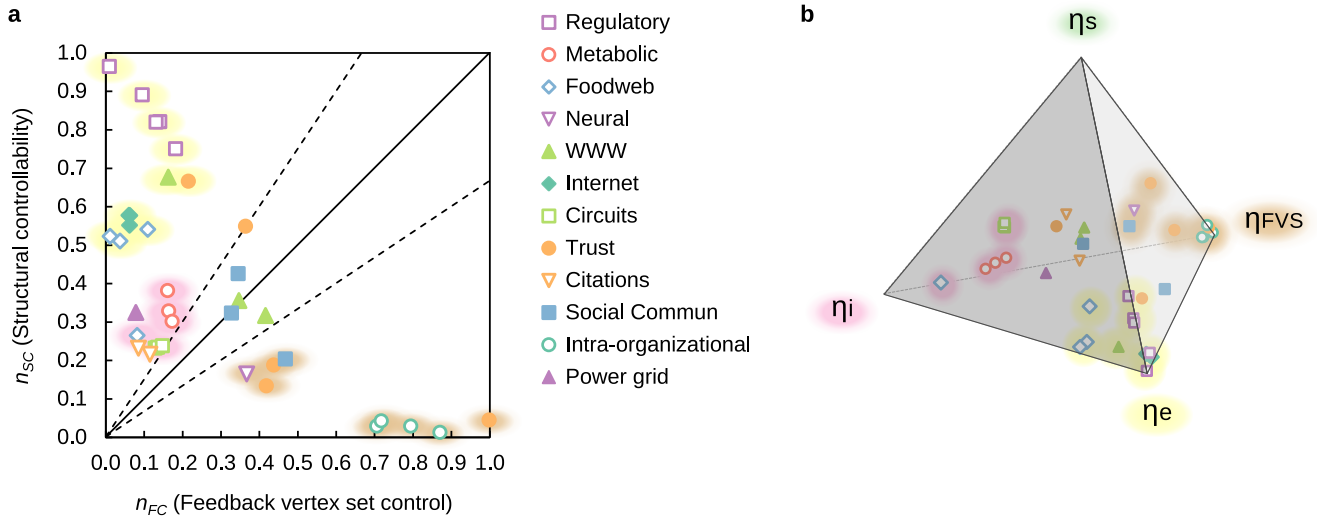


Fig. S7: Structure-based control in real networks. (a) Scatter plot with the fraction of control nodes in feedback vertex set (FVS) control ( $n_{FC}$ ) and structural controllability ( $n_{SC}$ ) for each real network in Table S1. The bold line denotes the positions in the plot with  $n_{SC} = n_{FC}$ , while the dashed lines denote  $n_{SC} = 1.5 n_{FC}$  and  $n_{FC} = 1.5 n_{SC}$ . The shading of the symbols corresponds to their position in panel b. (b) Barycentric plot of the normalized fraction of control nodes  $\eta_x$ , where  $x = s, e, i, FVS$  for each real network. The position in the plot is determined by  $\eta_x$  in such a way that a point is close to the  $\eta_x$  vertex if  $\eta_x \simeq 1$  and close to the face opposite to the  $\eta_x$  vertex if  $\eta_x \simeq 0$ . Thus, networks dominated by their FVS and strongly connected component are close to the  $\eta_{FVS}$  vertex (brown shading), networks dominated by their out-component are close to the  $\eta_e$  vertex (yellow shading), and networks dominated by internal dilations are close to the  $\eta_i$  vertex (pink shading). Networks dominated by their in-component would be close to the  $\eta_s$  vertex (green shading), but none of the networks are.

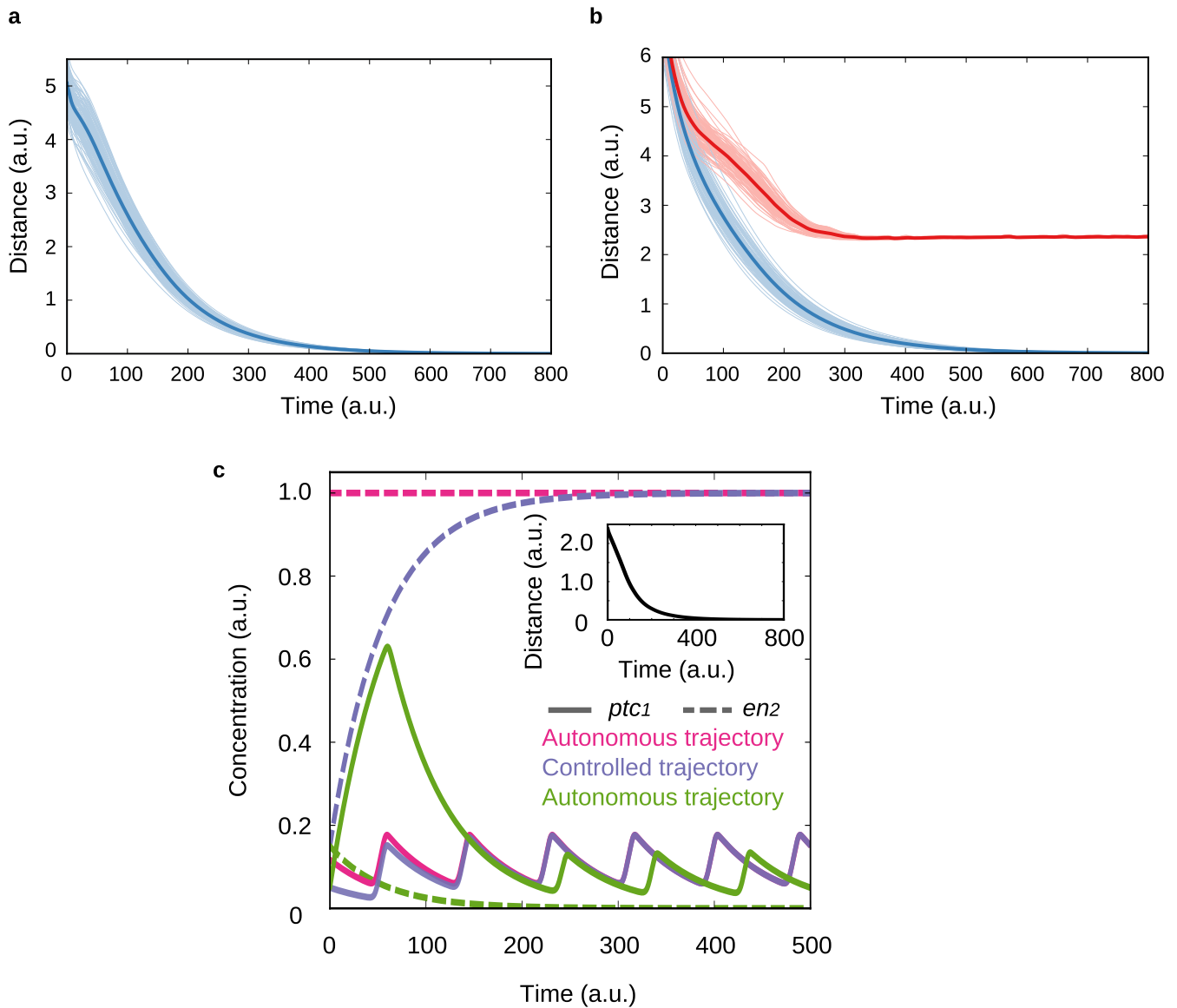


Fig. S8: Control of the Drosophila segment polarity gene differential equation model for a different parameter set than that used to generate Fig. 4. (a) The thin light blue lines show the evolution of the norm of the difference between the wild type attractor and the controlled state trajectory using FC for 100 randomly chosen initial conditions. (b) The thin light blues lines are the evolution of the norm of the difference between the wild type attractor and the controlled state trajectory using reduced feedback FC for 100 randomly chosen initial conditions. The thin red lines are the evolution of the norm of the difference between the wild type attractor and uncontrolled trajectory using reduced FC for 100 randomly chosen initial conditions. In all initial conditions the concentration of each quantity is chosen uniformly from the interval  $[0,1]$ . The thick blue(red) line is the average of the 100 realizations. (c) The concentration of *ptc* in the first cell (solid lines) and *en* in the second cell (dashed lines) with respect to time. Pink lines and green lines represent autonomous trajectories that start from different initial conditions (a wild type initial condition and a nearly null, respectively) and converge to different attractors (the wild type limit cycle and an unpatterned limit cycle, respectively). Blue lines represent the case when the system starts from the nearly null initial condition, and after applying FC, evolves into the wild type limit cycle. Inset: evolution of the norm of the difference between the desired attractor and the controlled state trajectory using FC.

Table S1: Network and control properties of the real networks analyzed. For each network, we show its number of nodes ( $N$ ), number of directed edges ( $M$ ), the fraction of feedback vertex set control (FC) nodes ( $n_{FC}$ ), the fraction of feedback vertex set nodes ( $n_{FVS}$ ), the fraction of source nodes ( $n_s$ ), the fraction of nodes in a strongly connected component (SCC) ( $n_{SCC}$ ), the normalized fraction of nodes in a SCC ( $\eta_{SCC}$ ), in the out-component of all SCCs ( $\eta_{out}$ ), and in the in-component of all SCCs ( $\eta_{in}$ ), the sum of the cycle number z-scores, the average fraction of FC nodes in degree-preserving randomized networks ( $n_{FC}^{Rand-Deg}$ ), in SCC-preserving randomized networks ( $n_{FC}^{Rand-SCC}$ ), and in short-cycle-preserving randomized networks ( $n_{FC}^{Rand-Cyc}$ ). The second page of the table shows the number of 1-cycles, 2-cycles, and 3-cycles in real networks, and the mean and standard deviation (S.D.) of the cycle numbers in degree-preserving randomized networks. The z-score of each cycle number is calculated using  $(C_L^{Real} - C_L^{Rand})/\sigma_{C_L}$ , where  $C_L^{Real}$  is the number of L-cycles in the real network,  $C_L^{Rand}$  is the mean number of cycles in degree-preserving randomized networks, and  $\sigma_{C_L}$  is the standard deviation of the number of cycles. The third page of the table shows the number of 4-cycles, the mean and standard deviation (S.D.) of 4-cycles in degree-preserving randomized networks, the fraction of nodes to be controlled under structural controllability (SC) ( $n_{SC}$ ), the fraction of external nodes ( $n_e$ ), the fraction of internal nodes ( $n_i$ ), the normalized fraction of feedback vertex set ( $\eta_{FVS}$ ), source ( $\eta_s$ ), external ( $\eta_e$ ), and internal ( $\eta_i$ ) control nodes, and the average fraction of FC nodes in fully randomized (Erdős-Rényi) networks ( $n_{FC}^{Rand-ER}$ ). (\*) The cycle z-score is larger than the number shown; the number of cycles in the real network exceeded  $2 \times 10^6$ . (\*\*) The maximum cycle length used was 3 instead of 4 because of the large number of cycles in both the real and randomized networks.

Type	Name	$N$	$M$	$n_{FC}$	$n_{FVS}$	$n_s$	$n_{SCC}$	$\eta_{SCC}$	$\eta_{out}$	$\eta_{in}$	$n_{FC}^{Rand-deg}$	$n_{FC}^{Rand-SCC}$	$n_{FC}^{Rand-Cyc}$	Cycle z-score
Regulatory	TRN Yeast 1	4441	12873	0.009	0.002	0.007	0.014	0.014	0.978	0.009	0.010	0.010	0.010	1.2
	TRN Yeast 2	688	1079	0.141	0.001	0.140	0.004	0.005	0.849	0.146	0.140	0.141	0.141	13.1
	TRN E coli 1	1550	3340	0.095	0.062	0.033	0.063	0.064	0.903	0.033	0.036	0.095	0.095	88.4
	TRN E coli 2	418	519	0.182	0.000	0.182	0.000	0.000	0.804	0.196	0.182	0.182	0.182	-0.3
	US-Corps Owner.	7253	6726	0.131	0.002	0.129	0.004	0.004	0.862	0.134	0.129	0.131	0.131	43.1
Metabolic	<i>E. coli</i>	2275	5763	0.161	0.138	0.023	0.940	0.940	0.036	0.024	0.071	0.161	0.146	40.4
	<i>S. cerevisiae</i>	1511	3833	0.164	0.136	0.028	0.939	0.939	0.032	0.028	0.082	0.164	0.145	34.6
	<i>C. elegans</i>	1173	2864	0.173	0.139	0.034	0.921	0.921	0.043	0.036	0.089	0.173	0.150	37.3
Neural	<i>C. elegans</i>	297	2345	0.367	0.276	0.091	0.818	0.821	0.084	0.095	0.324	0.369	0.429	19.8
Food web	Ythan	135	601	0.037	0.030	0.007	0.037	0.040	0.589	0.371	0.095	0.037	0.053	-14.5
	Seagrass	49	226	0.082	0.061	0.020	0.061	0.071	0.762	0.167	0.228	0.082	0.161	-12.7
	Grassland	88	137	0.011	0.000	0.011	0.000	0.000	0.972	0.028	0.028	0.011	0.020	-1.9
	Little Rock	183	2494	0.109	0.104	0.005	0.164	0.171	0.006	0.823	0.221	0.109	0.217	-23.1
WWW	Political blogs	1224	19025	0.346	0.217	0.130	0.664	0.663	0.197	0.140	0.295	0.347	0.349	149.3
	nd.edu	325729	1497134	0.164	0.164	0.000	0.386	0.388	0.612	0.000	0.114	0.160	0.161	21480.0*
	stanford.edu	281903	2312497	0.416	0.344	0.072	0.906	0.912	0.003	0.086	0.235	NA	NA	31790.4*
Internet	p2p-1	10876	39994	0.062	0.060	0.002	0.397	0.397	0.599	0.003	0.075	0.062	0.075	-4.4
	p2p-2	8846	31839	0.060	0.047	0.013	0.366	0.366	0.616	0.018	0.074	0.062	0.074	0.5
	p2p-3	8717	31525	0.062	0.053	0.009	0.370	0.374	0.623	0.003	0.072	0.064	0.072	4.5
Circuits	s838	512	819	0.129	0.063	0.066	0.299	0.392	0.515	0.092	0.098	0.129	0.138	52.0
	s420	252	399	0.135	0.063	0.071	0.306	0.397	0.500	0.103	0.111	0.135	0.145	25.7
	s208	122	189	0.148	0.066	0.082	0.320	0.406	0.469	0.125	0.131	0.148	0.157	12.3
Powergrid	Texas	4889	5855	0.078	0.001	0.078	0.003	0.007	0.697	0.296	0.085	0.078	0.085	1.6
Trust	Slashdot	82168	948464	0.998	0.953	0.045	0.955	0.955	0.000	0.045	0.327	0.998	0.998	13951.8**
	Wikivote	7115	103689	0.215	0.074	0.141	0.183	0.183	0.667	0.151	0.213	0.218	0.218	116.4
	College student	32	96	0.438	0.281	0.156	0.719	0.719	0.000	0.281	0.363	0.438	0.435	5.4
	Prison inmate	67	182	0.418	0.358	0.060	0.806	0.806	0.119	0.075	0.210	0.418	0.418	23.8
	Epinions	75879	508837	0.364	0.159	0.205	0.458	0.459	0.330	0.211	0.365	0.361	0.361	2569.3**
Citations	Arxiv HepTh	27770	352807	0.115	0.017	0.098	0.282	0.356	0.279	0.365	0.273	0.190	0.280	-51.5
	Arxiv HepPh	34546	421578	0.085	0.016	0.069	0.379	0.427	0.241	0.332	0.242	0.173	0.247	-10.3
Social Commun.	UConline	1899	20296	0.328	0.308	0.019	0.687	0.687	0.294	0.019	0.214	0.328	0.328	318.3
	cellphone	36595	91826	0.468	0.392	0.076	0.845	0.849	0.070	0.081	0.184	0.468	0.468	23489.0
	emails	3188	39256	0.345	0.223	0.122	0.637	0.637	0.239	0.124	0.269	0.345	0.345	683.9
Organizational	Freemans-2	34	830	0.794	0.794	0.000	1.000	1.000	0.000	0.000	0.747	0.794	0.794	7.8
	Freemans-1	34	695	0.706	0.706	0.000	1.000	1.000	0.000	0.000	0.658	0.706	0.706	10.0
	Manufacturing	77	2228	0.870	0.857	0.013	0.987	0.987	0.000	0.013	0.705	0.870	0.870	141.4
	Consulting	46	879	0.717	0.674	0.043	0.935	0.935	0.000	0.065	0.703	0.717	0.717	45.0

Table S1: Continuation of Table S1.

Name	1-cycles Rand-Deg	1-cycles S.D. Rand-Deg	2-cycles real	2-cycles Rand-Deg	2-cycles S.D. Rand-Deg	3-cycles real	3-cycles Rand-Deg	3-cycles S.D. Rand-Deg
TRN Yeast 1	0.00	0.00	9	5.64	2.46	13	12.88	3.74
TRN Yeast 2	0.00	0.00	1	0.06	0.26	1	0.01	0.10
TRN E coli 1	1.89	1.17	10	1.75	1.21	4	1.91	1.39
TRN E coli 2	0.00	0.00	0	0.04	0.20	0	0.01	0.10
US-Corps Owner.	0.59	0.76	13	0.23	0.44	2	0.06	0.24
<i>E. coli</i>	0.00	0.00	136	75.80	7.59	0	495.03	43.76
<i>S. cerevisiae</i>	0.00	0.00	26	51.40	6.31	0	290.24	27.52
<i>C. elegans</i>	0.00	0.00	22	37.34	5.17	0	180.08	20.57
<i>C. elegans</i>	0.00	0.00	197	55.72	6.36	431	374.47	21.11
Ythan	5.20	1.99	1	15.69	3.11	0	47.75	9.54
Seagrass	3.86	1.79	0	7.70	1.99	0	19.28	4.67
Grassland	0.00	0.00	0	0.48	0.64	0	0.38	0.60
Little Rock	11.87	3.25	42	62.05	6.43	137	439.07	28.78
Political blogs	30.61	4.27	2307	503.63	16.84	18481	10460.88	270.00
nd.edu	0.00	0.00	379571	931.91	25.72	>2000000	26738.39	298.34
stanford.edu	0.00	0.00	319861	180.04	14.27	689426	2261.60	86.61
p2p-1	0.00	0.00	0	10.40	3.49	33	31.01	5.74
p2p-2	0.00	0.00	0	9.39	2.93	34	25.87	4.72
p2p-3	0.00	0.00	0	8.86	3.16	40	26.80	5.57
s838	0.00	0.00	0	1.18	1.05	40	1.17	1.22
s420	0.00	0.00	0	1.16	0.99	20	1.03	1.04
s208	0.00	0.00	0	1.00	1.07	10	0.96	0.99
Texas	0.00	0.00	0	1.05	0.91	3	0.72	0.83
Slashdot	91.51	8.49	365931	5962.44	76.51	493487	414775.30	2420.23
Wikivote	0.00	0.00	2927	920.15	28.06	41856	25782.50	543.22
College student	0.00	0.00	16	4.72	1.88	14	9.29	2.19
Prison inmate	0.00	0.00	40	4.68	2.46	28	8.71	2.50
Epinions	0.00	0.00	103097	2904.37	48.08	740310	146423.86	1223.13
Arxiv HepTh	20.67	3.73	483	222.24	16.10	522	3074.18	76.26
Arxiv HepPh	16.46	4.18	657	119.64	11.50	506	1251.04	34.53
UCIonline	0.00	0.00	6458	621.98	17.58	10932	14291.28	210.11
cellphone	0.00	0.00	34973	8.55	2.23	19803	26.77	5.57
emails	0.00	0.00	7399	691.00	13.65	37693	16924.00	191.38
Freemans-2	0.00	0.00	356	334.17	3.33	5416	5385.59	14.39
Freemans-1	0.00	0.00	280	251.33	3.39	3503	3466.83	16.74
Manufacturing	0.00	0.00	887	498.55	7.98	13706	10206.85	68.29
Consulting	21.26	2.44	327	213.97	5.23	3492	2804.78	35.27

Table S1: Continuation of Table S1.

Name	4-cycles <i>real</i>	4-cycles <i>Rand-Deg</i>	4-cycles <i>S.D.</i> <i>Rand-Deg</i>	$n_{SC}$	$n_e$	$n_i$	$\eta_{FVS}$	$\eta_s$	$\eta_e$	$\eta_i$	$n_{FC}^{Rand-ER}$
TRN Yeast 1	29	31.01	8.694	0.965	0.958	0.000	0.003	0.007	0.990	0.000	0.182
TRN Yeast 2	0	0.00	0.045	0.821	0.670	0.008	0.002	0.170	0.818	0.010	0.188
TRN E coli 1	1	2.28	1.866	0.891	0.858	0.000	0.065	0.035	0.900	0.000	0.164
TRN E coli 2	0	0.00	0.000	0.751	0.565	0.008	0.000	0.241	0.749	0.010	0.215
US-Corps Owner.	1	0.05	0.218	0.82	0.684	0.008	0.002	0.157	0.831	0.010	0.240
<i>E. coli</i>	21442	3896.90	400.365	0.382	0.005	0.353	0.265	0.045	0.010	0.680	0.169
<i>S. cerevisiae</i>	12587	1890.78	217.395	0.329	0.000	0.301	0.292	0.061	0.000	0.647	0.169
<i>C. elegans</i>	7483	982.10	132.627	0.302	0.000	0.268	0.315	0.077	0.000	0.608	0.167
<i>C. elegans</i>	1992	2794.97	158.065	0.165	0.000	0.074	0.626	0.206	0.000	0.168	0.454
Ythan	0	162.46	38.920	0.511	0.378	0.126	0.055	0.014	0.699	0.233	0.296
Seagrass	0	53.00	12.608	0.265	0.163	0.081	0.188	0.063	0.500	0.249	0.364
Grassland	0	0.21	0.454	0.523	0.386	0.125	0.000	0.022	0.739	0.240	0.213
Little Rock	393	3477.90	270.563	0.541	0.000	0.536	0.161	0.008	0.000	0.831	0.631
Political blogs	339454	237762.00	5362.960	0.356	0.061	0.164	0.379	0.227	0.107	0.287	0.654
nd.edu	>2000000	862849.50	7850.500	0.677	0.577	0.100	0.105	0.000	0.762	0.133	0.286
stanford.edu	>2000000	31871.60	1348.996	0.317	0.000	0.244	0.000	0.228	0.000	0.772	0.474
p2p-1	85	102.96	10.251	0.552	0.544	0.006	0.098	0.003	0.890	0.009	0.225
p2p-2	105	85.58	9.819	0.578	0.551	0.012	0.075	0.021	0.885	0.019	0.220
p2p-3	137	85.66	10.335	0.577	0.562	0.006	0.085	0.014	0.892	0.009	0.221
s838	23	1.25	1.023	0.232	0.000	0.153	0.222	0.235	0.000	0.543	0.189
s420	11	1.18	1.135	0.234	0.000	0.161	0.214	0.241	0.000	0.545	0.198
s208	5	1.00	0.970	0.238	0.000	0.169	0.207	0.259	0.000	0.534	0.207
Texas	1	0.96	1.086	0.325	0.145	0.103	0.003	0.238	0.444	0.315	0.213
Slashdot	>2000000	>2000000	NA	0.045	0.000	0.000	0.955	0.045	0.000	0.000	0.774
Wikivote	1104831	790962.00	20559.181	0.666	0.524	0.000	0.100	0.191	0.709	0.000	0.638
College student	9	18.07	3.362	0.188	0.000	0.032	0.599	0.333	0.000	0.068	0.262
Prison inmate	24	16.68	4.292	0.134	0.045	0.030	0.728	0.121	0.091	0.060	0.211
Epinions	>2000000	>2000000	NA	0.549	0.110	0.236	0.224	0.288	0.155	0.332	0.407
Arxiv HepTh	2498	48068.08	1164.529	0.216	0.068	0.051	0.074	0.419	0.290	0.218	0.604
Arxiv HepPh	870	14502.94	324.466	0.232	0.114	0.049	0.064	0.279	0.459	0.198	0.593
UClonline	383109	367359.50	6481.181	0.323	0.270	0.036	0.487	0.031	0.426	0.056	0.550
cellphone	41349	83.57	9.706	0.204	0.000	0.128	0.657	0.128	0.000	0.214	0.169
emails	816457	461084.20	4226.713	0.426	0.116	0.188	0.343	0.188	0.179	0.290	0.593
Freemans-2	95082	95285.99	235.406	0.029	0.000	0.029	0.965	0.000	0.000	0.035	0.846
Freemans-1	52347	52531.32	276.189	0.029	0.000	0.029	0.961	0.000	0.000	0.039	0.795
Manufacturing	275530	229977.75	1098.990	0.013	0.000	0.000	0.985	0.015	0.000	0.000	0.805
Consulting	47296	40089.76	613.150	0.043	0.000	0.000	0.939	0.061	0.000	0.000	0.792

Table S2: Summary statistics of the distribution of  $n_{FVS}$  for real networks using different algorithms. We use two algorithms: the GRASP algorithm [9, 10] (GRASP) and the simulated annealing algorithm of ref. [11] (SA). For the GRASP algorithm we use the default parameters, and for the simulated annealing algorithm we use the same parameters as in [11] except for a  $maxMvt$  value between 0.05-5 times  $N$  (the network size) for the inner loop iteration parameter. The number of iterations for GRASP is 2000 for most networks and 50 for some of the largest networks (nd.edu, Slashdot, Epinions, Arxiv HepPh, Arxiv HepTh, and cellphone networks). The number of iterations for SA is between 10 and 100 per network.

Method	GRASP				SA			
	Name	$min n_{FVS}$	$median n_{FVS}$	$mean n_{FVS}$	$S.D. n_{FVS}$	$min n_{FVS}$	$median n_{FVS}$	$mean n_{FVS}$
TRN Yeast 1	0.002	0.002	0.003	0.000	0.002	0.002	0.002	0.000
TRN Yeast 2	0.001	0.001	0.001	0.000	0.001	0.001	0.001	0.000
TRN E coli 1	0.062	0.062	0.062	0.000	0.062	0.062	0.062	0.000
TRN E coli 2	0.000	0.000	0.000	0.000	0.000	0.000	0.000	0.000
US-Corps Owner.	0.002	0.002	0.002	0.000	0.002	0.002	0.002	0.000
<i>E. coli</i>	0.138	0.138	0.138	0.000	0.140	0.140	0.140	0.000
<i>S. cerevisiae</i>	0.136	0.136	0.136	0.000	0.137	0.138	0.138	0.001
<i>C. elegans</i>	0.139	0.139	0.139	0.001	0.142	0.142	0.142	0.000
<i>C. elegans</i>	0.283	0.283	0.283	0.000	0.269	0.273	0.275	0.003
Ythan	0.030	0.030	0.030	0.000	0.030	0.030	0.030	0.000
Seagrass	0.061	0.061	0.061	0.000	0.061	0.061	0.061	0.000
Grassland	0.000	0.000	0.000	0.000	0.000	0.000	0.000	0.000
Little Rock	0.104	0.104	0.104	0.000	0.104	0.104	0.104	0.000
Political blogs	0.217	0.219	0.220	0.005	0.217	0.217	0.217	0.000
nd.edu	0.160	0.160	0.160	0.000	0.161	0.161	0.161	0.000
stanford.edu	NA	NA	NA	NA	NA	NA	NA	NA
p2p-1	0.060	0.062	0.064	0.008	0.056	0.056	0.056	0.000
p2p-2	0.047	0.049	0.051	0.006	0.044	0.045	0.045	0.000
p2p-3	0.053	0.056	0.057	0.007	0.048	0.049	0.049	0.000
s838	0.063	0.063	0.063	0.000	0.063	0.063	0.063	0.001
s420	0.063	0.063	0.063	0.000	0.063	0.063	0.064	0.000
s208	0.066	0.066	0.066	0.000	0.066	0.066	0.066	0.000
Texas	0.001	0.001	0.001	0.000	0.001	0.001	0.001	0.000
Slashdot	0.953	0.953	0.953	0.000	0.953	0.953	0.953	0.000
Wikivote	0.074	0.076	0.077	0.003	0.074	0.075	0.075	0.000
College student	0.281	0.281	0.281	0.000	0.281	0.281	0.281	0.000
Prison inmate	0.358	0.358	0.361	0.006	0.358	0.358	0.358	0.000
Epinions	0.156	0.156	0.156	0.000	0.156	0.156	0.156	0.000
Arxiv HepTh	0.015	0.015	0.016	0.002	0.027	0.028	0.028	0.001
Arxiv HepPh	0.016	0.016	0.016	0.000	0.024	0.024	0.024	0.000
UCIonline	0.308	0.309	0.309	0.001	0.308	0.309	0.309	0.000
cellphone	0.392	0.392	0.392	0.000	0.391	0.391	0.391	0.000
emails	0.223	0.223	0.223	0.001	0.223	0.223	0.223	0.000
Freemans-2	0.794	0.824	0.827	0.026	0.794	0.794	0.794	0.000
Freemans-1	0.706	0.735	0.742	0.020	0.706	0.706	0.706	0.000
Manufacturing	0.857	0.857	0.863	0.010	0.857	0.857	0.857	0.000
Consulting	0.674	0.674	0.691	0.029	0.674	0.674	0.674	0.000

Table S3: Table comparing the control properties of feedback vertex set control (FC) and structural controllability (SC).

Control property \ Control method	Feedback vertex set control (FC)	Structural controllability (SC)
Dynamics	Dissipative nonlinear dynamics	Linear dynamics or linearized nonlinear dynamics
Control objective	Attractor control; any initial state to any target dynamical attractor	Full control; any initial state to any target state (linear case) or local control around a steady state or system trajectory (nonlinear case)
Control action	Node state variable override, overridden node states are specified; a controller signal $u(t)$ is not determined or guaranteed to exist	Controller signal $u(t)$ is guaranteed to exist; controller signal $u(t)$ is not explicitly determined

## SI TEXT

## I. Feedback vertex set control

## I.A. Previous work on feedback vertex set control

In [1, 2], Mochizuki, Fiedler et al. introduced the mathematical framework underlying feedback vertex set control (FC). Here we give a brief overview of the main concepts and results of [1] and its relation the work presented here. In the following  $X_i(t)$ ,  $i = 1, 2, \dots, N$ , denotes the state of the variable associated to node  $i$  at time  $t$ , and  $\mathbf{X} = (X_1, X_2, \dots, X_N)$  is a vector composed of the state of the variables of the network. In addition, we use  $X_J$  to denote  $X_j$  where  $j \in J \subseteq \{1, 2, \dots, N\}$ .

Let each of the system's node states  $X_i(t)$  evolve in time according to the differential equations

$$\frac{dX_i}{dt} = F_i(X_i, X_{I_i}, t), \quad i = 1, 2, \dots, N, \quad (\text{S1})$$

where  $F_i(X_i, X_{I_i}, t)$  encodes the network structure;  $I_i$  defines the predecessor (regulator) nodes of node  $i$  in the network and is such that self-loops are included in  $I_i$  only if the self-interaction is positive (i.e.,  $I_i$  contains node  $i$  only if  $\partial F_i/\partial X_i \geq 0$ ). In other words, negative self-regulation ( $\partial F_i/\partial X_i < 0$ ) is not included in  $I_i$ , only positive self-regulation is <sup>1</sup>. Furthermore, the  $F_i$ 's must depend negatively on the first argument of  $X_i$  (i.e., they must satisfy the decay condition  $\partial_1 F_i(X_i, X_{I_i}, t) < 0$ , where  $\partial_1$  indicates the partial derivative with respect to the  $X_i$  argument but not the  $X_{I_i}$  argument). Additionally,  $F_i$  and its first derivatives are assumed to be continuous functions and are assumed to be such that  $\mathbf{X}(t)$  is bounded ( $|\mathbf{X}(t)| < C$  for some constant  $C$ ) for any finite initial condition  $\mathbf{X}(t_0)$  and for all  $t \geq t_0$ , including the limit  $t \rightarrow \infty$ . Note that Eq. S1 determines the dynamics of all node variables, including source nodes, which stands in contrast to Eqs. 1-2 in the main text (Eqs. S3-S4). We consider the more general case of Eqs. 1-2 in Section I.B.

The boundedness conditions listed in the previous paragraph makes this system a so-called dissipative dynamical system, and guarantee that any initial state will converge to a global attractor  $\mathcal{A}$  as  $t \rightarrow \infty$ ,

$$\mathcal{A} = \left\{ \mathbf{X}(0) \mid \sup_{t \in \mathbb{R}} |\mathbf{X}(t)| < \infty \right\}. \quad (\text{S2})$$

<sup>1</sup> Note that considering only positive self-regulation as part of  $I_i$  is equivalent to adding a new auxiliary variable  $\zeta_i$  to encode for positive self-regulation (if any) and not including  $i$  as part of  $I_i$ . In other words, if  $\partial F_i/\partial X_i \geq 0$  with  $i \notin I_i$ , then we introduce  $\zeta_i = X_i$  and set  $\tilde{F}_i = F_i(\zeta_i, X_{I_i}, t) + \zeta_i - X_i$  as the new equation for node  $i$ . This would make  $\partial \tilde{F}_i/\partial X_i < 0$  for the expanded system and would make the feedback vertex set of the expanded system always include  $X_i$  or  $\zeta_i$ . This approach of adding an auxiliary variable is used in [1, 2].

The global attractor  $\mathcal{A}$  is bounded and invariant under Eq. S1, and contains all bounded dynamical attractors: steady states, limit cycles, quasi-periodic orbits, and bounded chaotic trajectories.

For the system we consider, the following theorem (Theorem 1.3 in [1]) forms the basis of FC:

*Theorem. Consider a differential equation system governed by Eq. S1 with dissipative functions  $F_i$ , and the associated directed graph  $G$  obtained from the  $I_i$ . We also assume  $F_i$  and its derivatives to be continuous. Moreover,  $G$  can contain a self-loop only if  $F_i$  does not satisfy the decay condition  $\partial F_i/\partial X_i < 0$ . Then a possibly empty subset  $J \subseteq \{1, 2, \dots, N\}$  of vertices of  $G$ , and any two solutions  $\mathbf{X}$  and  $\tilde{\mathbf{X}}$  of Eq. S1 satisfy*

$$\lim_{t \rightarrow \infty} (X_J(t) - \tilde{X}_J(t)) \rightarrow 0 \quad \text{implies} \\ \lim_{t \rightarrow \infty} (\mathbf{X}(t) - \tilde{\mathbf{X}}(t)) \rightarrow \mathbf{0}$$

for all choices of nonlinearities  $F_i$  if and only if  $J$  is a feedback vertex set (FVS) of the graph  $G$ .

A consequence of this theorem is that a system governed by Eq. S1 with an empty FVS must have any pair of solutions approach each other as  $t \rightarrow \infty$ , i.e., there is single dynamical attractor. Now, if we take a system with a non-empty FVS and override the node state variables of its FVS with their value in the trajectory of any of its dynamical attractors  $\mathcal{D}$ , then the overridden system is equivalent to a system with an empty FVS <sup>2</sup>. Since the dynamical attractor  $\mathcal{D}$  is still a dynamical attractor of the overridden system, which has an empty FVS, it must be the only dynamical attractor of the overridden system. Hence, if we override the dynamics of the FVS of system Eq. S1 with the trajectory in one of its dynamical attractors, this theorem guarantees that the overridden system will converge to this attractor. Furthermore, overriding the full FVS is necessary and sufficient if one wants this control action to hold for all choices of  $F_i$ 's.

The FVS framework does not predict what happens when the node state override is close to but not precisely at the prescribed state (likely because this could be model-dependent and attractor-dependent). In general, the expectation is that a node state override that mimics the desired state as closely as possible will move the system into the basin of attraction of the desired attractor and the system will thus converge into the desired attractor.

<sup>2</sup> Let  $J \subseteq \{1, 2, \dots, N\}$  be the node indices of a FVS, and let  $K = \{1, 2, \dots, N\}/J$  be the node indices of nodes not in the FVS. The dynamics of nodes  $K$  in the overridden system are given by  $\dot{X}_k = F'_k(X_k, X_{I'_k}, t) = F_k(X_k, X_{I_k}, t) |_{X_J(t)=X_J^{\mathcal{D}}(t)}$ ,  $k \in K$ , where  $X_J^{\mathcal{D}}(t)$  is the trajectory of the overridden node states. Since  $F'_k(X_k, X_{I'_k}, t) = F_k(X_k, X_{I_k}, t) |_{X_J(t)=X_J^{\mathcal{D}}(t)}$ , then  $I'_k$  does not contain any node in  $J$  and the graph defined by the  $I'_k$  will have no cycles (removing  $J$ , by definition, makes the graph acyclic).

### I.B. Feedback vertex set control for general system dynamics

Consider the general system used in the main text. The state of the system's  $N$  nodes at time  $t$ , characterized by source node variables  $S_j(t)$  (for nodes with no incoming edges) and internal node variables  $X_i(t)$ , obeys the equations

$$\frac{dX_i}{dt} = F_i(X_i, X_{I_i}, t), \quad i = 1, 2, \dots, N - N_s, \quad (\text{S3})$$

$$\frac{dS_j}{dt} = G_j(t), \quad j = N - N_s + 1, \dots, N, \quad (\text{S4})$$

The dynamics of each source node  $j$  is independent of the internal node variables  $X_i$  (by definition), and is fully determined by  $G_j(t)$ , and does not include a decay term. In the simplest case  $G_j = 0$  and  $S_j$  will remain in the specified initial state. The dynamics of each internal node  $i$  is governed by  $F_i(X_i, X_{I_i}, t)$ , where the  $I_i$  determines the predecessor nodes of  $i$  (which can be source or internal nodes) and satisfies the same conditions as in Section I.A. The dynamics are assumed to be bounded, and the  $F_i$ 's and  $G_j$ 's and their first derivatives are taken to be continuous.

For this system, the theorem in Section I.A and its consequences (i.e., the results of refs. [1, 2]) cannot be applied directly since the source node variables  $S_j(t)$  do not obey Eq. S1. Note that the addition of the source node variables  $S_j$  is not merely cosmetic; the  $S_j$ 's can denote external stimuli the system is subject to or initial-condition-specified node variables (as would happen if  $G_j = 0$ ); these stimuli or initial/boundary variables can affect the dynamical attractors available to the system (e.g. steady states can merge or disappear if  $S_j$  takes different values, see e.g. [3, 4]).

Here we adapt the previous results of feedback vertex set control to the more general system dynamics. Let  $\mathcal{D}$  be the desired dynamical attractor and let  $S_j^{\mathcal{D}}(t)$  be the source node trajectory in which this attractor is obtained. Now, assume that the system's source nodes are driven by an arbitrary  $G_j(t)$ . If starting at time  $t_0$ , we override the state of the source nodes  $S_j(t)$  with  $S_j^{\mathcal{D}}(t)$ , then for  $t > t_0$  we will have  $S_j(t)$  be in their state in  $\mathcal{D}$ . Additionally, the dynamics of the  $X_i$  for  $t > t_0$  can be described by  $\dot{X}_i = F_i(X_i, X_{I_i}, t) = F_i |_{S_j(t)=S_j^{\mathcal{D}}(t)}$ , where the  $F_i$ 's no longer depend on  $S_j$  (i.e.,  $I_i$  is  $I_i$  with all the  $S_j$  removed). Since the dynamics of the modified system now obey Eq. S1 (with  $F_i'$  instead of  $F_i$ ), then we can guarantee that the *FVS* can be used to steer the system to any dynamical attractor of interest. Finally, since  $F_i' = F_i |_{S_j(t)=S_j^{\mathcal{D}}(t)}$ , then  $\mathcal{D}$  is one of the attractors of the modified system ( $\dot{X}_i = F_i'$  and  $\dot{X}_i = F_i$  with  $S_j(t) = S_j^{\mathcal{D}}(t)$  both have the same governing equations). The result is that the overriding the state of the source nodes  $S_j$  and of the *FVS* into the state in a dynamical attractor  $\mathcal{D}$  is guaranteed to steer the system to  $\mathcal{D}$  as  $t \rightarrow \infty$ .

As an example, consider the network in Fig. S1a, and

the governing equations:

$$\frac{dS}{dt} = G_S, \quad (\text{S5})$$

$$\frac{dX}{dt} = k_x(Z - \alpha_x X), \quad (\text{S6})$$

$$\frac{dY}{dt} = S + \frac{X + Z}{1 + k_S S} - \alpha_Y Y, \quad (\text{S7})$$

$$\frac{dZ}{dt} = \beta_Z + \frac{X^2}{X^2 + 1} - \alpha_Z Z Y, \quad (\text{S8})$$

where  $G_S = 0$ ,  $k_x = 10$ ,  $\alpha_x = 0.5$ ,  $k_S = 5$ ,  $\alpha_Y = 0.2$ ,  $\beta_Z = 0.01$ , and  $\alpha_Z = 0.2$ . Under these conditions, the system has several attractors, including a limit cycle (Fig. S1b, Attractor 1) and a steady state (Fig. S1b, Attractor 2). FC guarantees that for either of these two attractors, and any others that exist, the control action of overriding the state variables of the FC node set into the trajectory of a target attractor guarantees that any initial state will converge to said attractor. This means that forcing  $S$  and  $Z$  into the trajectory specified by Attractor 1 guarantees that the rest of the system ( $X$  and  $Y$ ) will converge to Attractor 1, and the same is true for any target attractor Fig. S1c. Furthermore, if one modifies the parameters or the functional form of the equations of the system, forcing  $S$  and  $Z$  into the trajectory of an attractor of the modified system guarantees that the modified system will converge to the modified attractor (as long as the modified system is still a dissipative nonlinear system).

### I.C. Identifying the minimal feedback vertex set control set of a network

The FC node set of a network of  $N$  nodes is composed of the source nodes of the network ( $N_s$  of them) and of the FVS of the network. The minimal FC node set  $N_{FC}$  of a network is obtained by finding a minimal FVS, since the number of source nodes  $N_s$  is fixed for any given network. The minimal FVS of a network is not guaranteed to be unique, and is often found to have a large degeneracy (see the examples in Fig. 1 of the main text).

In order to find the minimal FVS control set of a network, we must find which of the possible  $2^{N-N_s}$  node sets is a minimal FVS. The problem of identifying the minimal FVS has a long history in the area of circuit design [5]. Even though solving the minimal FVS problem exactly is NP-hard [6], a variety of fast algorithms exist to find close-to-minimal solutions [5, 7]. Here we use the FVS adaptation of a heuristic algorithm known as the greedy randomized adaptive search procedure (GRASP) [8], which is commonly used for combinatorial optimization problems [5]. GRASP is an iterative procedure in which each iteration consists of two phases: a construction phase in which a feasible solution to the problem is produced based on a greedy measure and a randomized selection process (given a cutoff for the greedy measure, a feasible solution below the cutoff is chosen randomly

and uniformly), and a local search phase in which the local neighborhood in the space of solutions is explored to find a local minimum of the problem. The FVS adaptation of GRASP incorporates the wiring diagram of the network into the procedure by using the in-degree and out-degree of each node as the greedy measure in the construction phase and by utilizing a graph reduction technique that preserves the FVS during the local search phase [9, 10]. In addition, we preprocess all networks by iteratively removing source and sink nodes (this is done iteratively because new source/sink nodes may appear after a source/sink node is removed), since a minimal  $FVS$  of a network is invariant under removing nodes that do not participate in directed cycles.

For this work, we use a custom code in Python to iteratively remove source and sink nodes in each network analyzed. The resulting network is then used as an input to the FORTRAN implementation of the FVS adaptation of GRASP [9, 10] using the default settings (2048 iterations and a random uniformly chosen cutoff for the randomized selection process in each iteration), unless otherwise noted.

The NP-hardness of the minimal FVS problem is a limitation of FC, given the approximate nature of any algorithm that can be used on large networks. To evaluate our confidence in the minimal FVS we obtained with the GRASP algorithm [9, 10], we characterized the distribution of outcomes in all networks (except for the stanford.edu network due to time and resource limitations). The almost identical  $n_{FVS}$  obtained using either the minimal or the median result of all iterations (Table S2) indicates that increasing the number of iterations of the GRASP algorithm would have a small effect on our results. In addition, we also use another algorithm to solve the minimal FVS problem, a simulated annealing algorithm with a novel local search procedure [11]. The resulting  $n_{FVS}$ 's are almost identical (Table S2), which indicates that our results are not method-dependent. The consistency between these results greatly increases the confidence in the  $n_{FVS}$ 's we obtained with the GRASP algorithm.

#### *I.D. Feedback vertex set control and model-based network control*

Feedback vertex set control gives a set of nodes whose control is sufficient for attractor control in the ensemble of all models that have a given network structure. This set of nodes is also necessary if one demands that control of the same node set be sufficient in every model of the ensemble. Thus, FC gives a sufficiency prediction about the entire ensemble of models with a given network structure, and any particular model in the ensemble may require a smaller set of nodes for attractor control (i.e. the FC node set gives an upper bound for any particular model). Consequently, a subset of the FC node set of a network can often be sufficient for a particular instance

of a model with this underlying network structure (section “Feedback vertex set control and dynamic models of real systems” of the main text). The generality of this result is supported by a recently developed network control method for Boolean dynamic models called stable motif control [12].

Stable motif control is an attractor-based control method that is based on identifying subnetworks which uniquely determine an attractor of interest. Specifically, stable motif control identifies a state manipulation of certain nodes in the subnetworks (namely, fixing them in their states in the desired attractor) that drives any initial state to the desired attractor with 100% effectiveness [12]. Stable motif control and feedback vertex set control differ in the dynamic variables they consider (Boolean vs continuous<sup>3</sup>) and the information they require (model-based vs structure-based), but they share their attractor-based control objective and their ability to drive any initial state to a desired attractor. Additionally, they share specific methodological aspects:

- (i) In stable motif control, source nodes are assumed to be fixed in the node state specified by the attractor of interest; if this were not the case, the source nodes would first need to be fixed into the appropriate node state. In FC, source nodes must also be locked in the trajectory specified by the attractor.
- (ii) In stable motif control, each subnetwork identified is either a self-sustaining positive feedback loop (directed cycle), or an intersection of several self-sustaining positive feedback loops. In FC, every feedback loop in the network (both positive and negative) must be manipulated, something which is achieved using an override of the states of the feedback vertex set, which by definition contains a node in every feedback loop in the network.

The first point shows that the treatment of source nodes is almost identical in both methods, and that FC is more general because it allows source nodes to be in any dynamical trajectory and not only a fixed node state, like in stable motif control. The second point shows that the state manipulation of cycles underlies both methods, and that FC requires manipulating all cycles while stable motif control only requires manipulation of a select

---

<sup>3</sup> Boolean dynamics are a type of nonlinear and dissipative dynamics, which assume two discrete node states, and which can be considered a limiting case of sigmoidal regulatory functions often observed in biological systems, for example, Hill functions with a large Hill coefficient. Boolean dynamics require feedback loops for multi-stability or oscillatory behavior, which guarantees that an acyclic Boolean network (which is equivalent to what we obtain when overriding the state of the FVS) has a unique attractor [13]. This is sufficient to guarantee that FC implies attractor control if the FC nodes are fixed (i.e. do not oscillate) in the attractor of interest, but it is not clear if this also extends to oscillating nodes.

few positive cycles. The similarities in points (i) and (ii) strongly suggest that stable motif control is the model-based equivalent of feedback vertex set control for the case of Boolean dynamics. In particular, point (ii) gives an explanation of why a reduced FVS can often be sufficient for FC; even though all cycles must be controlled in structure-based control, in a particular model instance only a subset of the cycles (and thus, a subset of the FVS) is sufficient for attractor-based control.

### *I.E. Feedback Vertex Set control and self-dynamics*

In FC, the graph structure (encoded in  $I_i$ ) only needs to consider positive self-loops. This means that FC benefits from knowing some information about the sign (regulatory effect) of self-interactions. Edge sign is otherwise not encoded in the graph structure. If the sign of a self-interaction is not known (or if it can change sign depending on the value of other regulators, as in the case of a logical XOR function), then the self-interaction needs to be included in the graph.

For the case of biological systems, one often knows the regulatory effect of self-interactions from biological evidence (e.g. the regulonDB transcriptional regulatory network in <http://regulondb.ccg.unam.mx/> contains the positive, negative or dual nature of interactions), and one can include this in the graph to increase the predictive power of FC. For other biological, social, or technological networks it might not be obvious whether self-interactions are positive, so one needs to choose whether such self-interactions can be positive (which would mean including such self-interactions in the graph) or can only be negative (in which case they do not need to be included in the graph).

### *I.F. Feedback vertex set control and controllers*

In feedback vertex set control we use the control action of forcing (overriding) the state variables into a certain trajectory, namely, the one specified by an attractor of the system we are interested in. The control action of state variable override in FC stands in contrast with the control actions often considered in control theory, in which a controller or driver signal  $u(t)$  is coupled to the governing equations  $F_i$  and  $G_j$ , and through this coupling are the trajectories of the state variables  $X_i$  and  $S_j$  modified. In the simplest case, known as control-affine systems, we would have  $\dot{X}_i = F_i + u_i(t)g_i(X, S)$  as the governing equation of the variable of the nodes  $i$  we chose to control (and similarly for the source node variables  $\dot{S}_j$ ).

The problem of designing a controller  $u(t)$  for nonlinear systems has been the subject of much research over the last decades (e.g. [14–16]), yet designing a controller for a general nonlinear system that drives an initial condition to a target attractor of the system (attractor-based control) is a difficult and unsolved problem (see e.g. sec-

tion V of the review in [15]). Recent efforts in attractor-based control require a parameterized model in order to be applicable (and, thus, are not structure-based methodologies) and rely on numerical simulations to design the controller [15]. For example, refs. [17] and [18] give algorithms to numerically obtain a controller (an infinitesimal change of the given initial condition in [17], or a temporary modification of parameters in [18]) that drives the system to the basin of attraction of a target attractor, and leads the system to this attractor

These examples of attractor-based control illustrate that designing a controller for a nonlinear system is a research endeavor of its own and seems to depend strongly on the dynamic model and its parameters. Given that our work focuses on the structure-based aspect of the attractor-control problem, we consider designing a controller to be outside the focus of our current work and a topic of future research. Having said this, the control action of node override can be viewed as an idealized controller signal that allows us to identify the nodes that need to be controlled in systems for which we do not have a parameterized dynamic model or know the system-specific coupling of the controller signal with the equations of motion (Eqs. S3-S4). Thus, override control is a necessary first step in the task of designing driver signals for these systems.

## II. Structural controllability

### *II.A. Notes on structural controllability*

In structural controllability (SC) we consider a system with an underlying network structure whose autonomous dynamics are governed by linear time-invariant ordinary differential equations

$$\frac{d\mathbf{x}}{dt} = A\mathbf{x}(t), \quad (\text{S9})$$

where  $\mathbf{x}(t) = (x_1(t), x_2(t), \dots, x_N(t))$  denotes the state of the system, and  $A$  is a  $N \times N$  matrix that encodes the network structure and is such that  $a_{ik}$  is nonzero only if there is a directed edge from  $k$  to  $i$ . Given this system, SC's aim is to identify external driver node signals  $\mathbf{u}(t) = (u_1(t), \dots, u_M(t))$  that can steer the system from any initial state to any final state in finite time (i.e., full control, Fig. S6a), and that are coupled to Eq. S9 in the following way

$$\frac{d\mathbf{x}}{dt} = A\mathbf{x}(t) + B\mathbf{u}(t), \quad (\text{S10})$$

where  $B$  is a  $N \times M$  matrix that describes which nodes are driven by the external signals  $\mathbf{u}(t)$ .

The work of Lin, Shields, Pearson, and others showed that if such a system can be controlled in the specified way by a given pair  $(A, B)$ , which can be verified using

Kalman’s controllability rank condition <sup>4</sup>, this will also be true for almost all pairs  $(A, B)$  (except for a set of measure zero) [14, 20, 21]. In other words, SC is necessary and sufficient for control of almost all linear time-invariant systems consistent with the network structure in  $A$ . The applicability of SC also extends to nonlinear systems; SC of the linearized nonlinear system around a steady state or system trajectory of interest is a sufficient condition for local controllability of the system around said steady state or trajectory in a sufficiently small time [14–16]. Furthermore, SC of the linearized nonlinear system is also a sufficient condition for some nonlinear notions of controllability such as accessibility [14–16].

SC is a mathematical formalization of the idea that a node can fully manipulate only one of its successor elements at a time and that a directed cycle is inherently self-regulatory. A consequence of this is that the driver nodes are such that every network node is either part of a set of non-intersecting linear chains of nodes that begin at the driver nodes or is part of a set of directed cycles that do not intersect each other or the set of linear chains and which are reachable from the driver nodes (Fig. S6). As Ruths & Ruths showed [22], this implies that there are three types of network nodes that must be directly manipulated by a unique driver node, and which we call SC nodes: (i) every source node, and every successor node of a dilation (when a node has more than one successor node) that is not part of the set of linear chains or of the cycles, namely (ii) the surplus of sink nodes with respect to source nodes or (iii) internal dilation nodes.

To illustrate how the nodes that need to be manipulated in SC and FC can differ from each other, consider the example networks in Fig. S6. In a linear chain of nodes (Fig. S6c, left) the only node that needs to be controlled in both frameworks is the source node  $S_1$ . For Fig. S6d, which consists of a source node connected to a cycle, SC requires controlling only the source node  $S_1$  since the cycle is considered self-regulating (Fig. S6d, middle), while FC additionally requires controlling any node  $X_i$  in the cycle, the feedback vertex set in this network (Fig. S6d, right). Fig. S6e consists of a source node with three successor nodes; SC requires controlling two of the three successor nodes because of the dilation at the source node  $S_1$ , while for FC controlling  $S_1$  is sufficient. In Fig. S6f we show a more complicated network with a cycle and several source and sink nodes, and two minimal node sets for SC and FC. These examples illustrate that the control of the source nodes is shared by full control in SC and attractor control in FC, and that their main difference is in the treatment of cycles, which require to be controlled in FC and do not require independent control in SC.

<sup>4</sup> Namely, that the  $N \times NM$  matrix  $(B, AB, A^2B, \dots, A^{N-1}B)$  has full rank, i.e.,  $\text{rank}(C) = N$  [19].

## II.B. Structural controllability and self-dynamics

In a system governed by Eq. S10, self-dynamics is captured by having the matrix elements in the diagonal of  $A$  be nonzero (i.e., a self-loop in the network structure). If each node variable in the system has self-dynamics, then every node in the associated graph structure of  $A$  will have a self-loop. Directly applying SC to such a graph will yield the surprising result that a single driver signal  $\mathbf{u}(t) = (u_1(t))$  is necessary and sufficient for full control, regardless of any other aspect of the graph structure [15, 23, 24]. This result, although mathematically correct, gives little insight into the impact of the underlying network structure of  $A$  (other than self-loops) on control-related questions. Furthermore, as Sun et al. showed using minimal-energy control driver signals <sup>5</sup>, the required driver signal  $\mathbf{u}(t) = (u_1(t))$  might be numerically impossible to implement unless the number of control nodes is significantly increased [25].

We should emphasize that controllability of a system with self-dynamics by a single driver signal is a consequence of SC’s assumption that each nonzero entry in  $A$  and  $B$  is independent of each other. Thus, if one considers SC for the set of  $(A, B)$ ’s in which the diagonal elements of  $A$  are fixed (i.e., the self-dynamics are fixed but every other nonzero entry is still arbitrary) then the number of driver nodes can be obtained from the eigenvalues of  $A$  and their geometric multiplicities <sup>6</sup>, as shown in a recent study by Zhao et al. [26]. For most cases, obtaining the eigenvalues of  $A$  and their geometric multiplicities is computationally demanding and requires specifying a value for the weight  $a_{ii}$  of each self-loop. For the special case of a single fixed weight  $\alpha$  for the self-dynamics of every node ( $a_{ii} = \alpha, \forall i$ ), the number of driver nodes is equivalent to the one specified by SC using  $A$  but setting all diagonal elements to zero [26].

These considerations about self-dynamics are crucial when using SC on the nonlinear systems we consider, Eqs. S3-S4. Since the nonlinear functions  $F_i$  have a decay term that prevents the system from increasing without bounds, then a linearization of the  $F_i$ ’s will give nonzero diagonal entries for  $A$ . Thus, SC would predict that a single driver signal is sufficient for controllability regardless of the topology of the real network considered, a result which tells us little about structure-based control in these networks. Instead, we follow the approach of Liu et al. [23] and do not include the decay self-dynamics as a self-loop in the graph structure. Two equivalent interpretations of this approach under SC are that (i) we consider the decay terms to not dominate the linearized dynamics (i.e., we set them to zero), or (ii) every ele-

<sup>5</sup> Minimal-energy control driver signals are the ones that minimize the functional  $\int_0^{t_f} \|\mathbf{u}(t)\|^2 dt$ , where  $t_f$  is the desired final time.

<sup>6</sup> The geometric multiplicity  $\mu(\lambda)$  of an eigenvalue  $\lambda$  of  $A$  is given by  $\mu(\lambda) = N - \text{rank}(\lambda I - A)$ , where  $I$  is the  $N \times N$  identity matrix.)

ment has the same (or very similar) fixed weight for its self-dynamics (i.e., the self-dynamics are fixed and every other nonzero entry in  $A$  is arbitrary).

### II.C. Identifying the minimum number of driver nodes in structural controllability

Here we use the maximum matching approach of Liu et al. [23] to identify the minimum number of driver nodes in  $SC$ . Given a directed network, an undirected bipartite graph is created in the following way: for every node  $i$  in the original network, a node  $i^+$  of type  $+$  and a node  $i^-$  of type  $-$  are created in the bipartite graph. The connectivity in the bipartite graph is such that if node  $i$  has a directed edge to node  $j$  in the original network, then the bipartite graph will have an undirected edge from node  $i^+$  to node  $j^-$ . As Liu et al. showed, a maximum matching of the bipartite graph (maximum number of edges with no common nodes) gives the minimum number of driver nodes in  $SC$ ; each node in the original network corresponding to a node of type  $+$  that is not in the maximum matching must be directly regulated by a driver node. A maximum matching of a graph is not unique, which implies that the set of nodes that must be directly regulated by a driver node is not unique either. The maximum matching of a bipartite graph can be efficiently found in  $O(\sqrt{NM})$  time using the Hopcroft-Karp algorithm.

For this work, we use a custom code in Python to implement the maximum matching approach of Liu et al. [23], and use the implementation of the Hopcroft-Karp algorithm in the Python package NetworkX (<https://networkx.github.io/>, version 1.10) to find the maximum matching.

### II.D. Comparing feedback vertex set control and structural controllability

Feedback vertex set control and structural controllability can both be used to answer the question of how difficult to control a network is, based solely on network structure, but they differ in the underlying dynamics they consider, their control objective, and their control actions. To be more specific:

- FC considers dissipative nonlinear dynamics, while SC considers linear dynamics or linearized nonlinear dynamics [15, 23].
- FC's control objective is attractor-control (from any initial state to any target system attractor) while SC's control objective is full control (from any initial state to any target state for linear dynamics, or among states near a steady state or system trajectory for nonlinear dynamics [15, 23]).
- FC provides what state or trajectory the selected nodes should follow, but not how or if an external driver signal  $u(t)$  (a controller) can make this happen. The existence of a driver signal  $u(t)$  is guaranteed in SC, although SC does not explic-

itly determine this  $u(t)$ , and one may need to add extra constraints if  $u(t)$  is required to have certain properties, e.g. the length of the linear chains of nodes spanned by each independent  $u(t)$  need to be shorter than a threshold to find a numerically implementable signal [25, 27].

- The external driver signal of SC is likely to be dependent on the initial state and on the target state, while the state/trajectory of the overridden nodes in FC only depends on the target attractor and is independent of the initial state (though, a controller for FC would likely be dependent on the initial condition).

We summarize the difference between these methods in Table S3. SC and FC are very different methods, so one should be careful about extending their predictions beyond their realm of applicability. Indeed, a lot of work has been done in using SC on networks which have inherently nonlinear dynamics and in which the questions asked use a notion of control that seem to be closer to attractor control (e.g. refs. [28–30], and some of the results from refs. [15, 23]). In these cases, the hope seemed to be that the network insights obtained from linear dynamics would be close enough to those of nonlinear dynamics even though SC made no such guarantee. The results of our work and others' [24, 31] caution against this.

## III. Structure-based control of real networks

### III.A. Real networks used in this study

Here we describe each network in Table S1, provide the reference where each network was first reported, and give the link to where the network was obtained (if publicly available). For many of these networks, the orientation of the directed edges does not match the expected direction of influence in a dynamic model; if there is an edge from node  $i$  to node  $j$ , we expect the state of node  $i$  to influence the state of node  $j$  (e.g., in an epidemic model, if individual  $i$  is infected and  $i$  can spread the disease to  $j$ , then we expect node  $j$  to get infected). For these networks, we follow [23] and [22], and reverse the orientation of the directed edges in order for it to match the expected directionality of influence.

- ***E. coli* transcription regulatory network 1 [32]**. Graph of the transcriptional regulation network in the bacterium *Escherichia coli*. Vertices denote genes; a gene that codes for a transcription factor that regulates the transcription of a target gene is denoted by a directed edge between them. The version of the network used was obtained directly from Yang-Yu Liu.
- ***E. coli* transcription regulatory network 2 [33]**. Graph of the transcriptional regulation network in the bacterium *Escherichia coli*. Operons (a gene or group of genes transcribed together) are denoted by vertices; an operon that codes for a transcription factor that directly regulates a target

- operon is denoted by a directed edge. This network was obtained from Hawoong Jeong's website <http://stat.kaist.ac.kr/index.php>.
- ***S. cerevisiae* transcription regulatory network 1 [34], 2 [35]**. Graph of the transcriptional regulation network in the yeast *Saccharomyces cerevisiae*. Genes are denoted by vertices; a gene that codes for a transcription factor that regulates a target gene is denoted by a directed edge between them. Network 1 was obtained from the supplemental information in ref. [34], and network 2 was obtained from Uri Alon's website <https://www.weizmann.ac.il/mcb/UriAlon/download/collection-complex-networks>.
  - **US corporate ownership [36]**. Graph of the ownership relations among companies in the telecommunications and media industries in the United States. Companies are denoted by vertices and ownership of a company by another is denoted by an edge originating from the owner company. This network was obtained from the Pajek network dataset <http://vlado.fmf.uni-lj.si/pub/networks/data/econ/Eva/Eva.htm>
  - ***E. coli*, *S. cerevisiae*, *C. elegans* metabolic networks [37]**. Graph of the metabolic network of the bacterium *Escherichia coli*, the yeast *Saccharomyces cerevisiae*, and the worm *Caenorhabditis elegans*. Substrates (molecules) and temporary complexes are denoted by vertices; substrates that participate as a reactant in the reaction associated to a complex have an edge to it, and substrates that are products of the reaction associated to a complex have an edge from it. These network were obtained from Hawoong Jeong's website <http://stat.kaist.ac.kr/index.php>.
  - ***C. elegans* neural network [38, 39]**. Graph of the *Caenorhabditis elegans* worm's neural network. Neurons are denoted by vertices and synapse/gap junctions between neurons are denoted by edges. This network was obtained from the UC Irvine Network Data Repository <http://networkdata.ics.uci.edu/data/celegansneural/>.
  - **Ythan [40, 41], Seagrass [41, 42], Grassland [41, 43], and Little Rock [41, 44] food web networks**. Graph of the predatory interactions among species in the Ythan Estuary, the St. Marks Seagrass, the England/Wales Grassland, and the Little Rock Lake. Every species is denoted by a vertex, and if a species preys on another species an edge is drawn from the prey to the predator. This network was obtained from the Cosin Project network data <http://www.cosinproject.eu/extra/data/foodwebs/WEB.html>.
  - **Political Blogs [45]**. Graph of the hyperlinks between blogs on US politics in 2005. Every blog is denoted by a vertex and hyperlinks are denoted by edges that point towards the linked blog. In this work we reverse the edges of this network so that they match the direction of influence in a dynamic model (i.e., if a blog has a hyperlink to another blog, then the latter influenced the former). This network was obtained from Mark Newman's website <http://www-personal.umich.edu/mejn/netdata/>.
  - **WWW network of stanford.edu [46] and nd.edu [47]**. Graph of the web networks of Stanford University (domain stanford.edu) and the University of Notre Dame (domain nd.edu). Every webpage is denoted by a vertex and hyperlinks are denoted by edges that point towards the linked webpage. This network was obtained from the Stanford Large Network Dataset Collection <https://snap.stanford.edu/data/>.
  - **Internet networks [48, 49]**. Graphs of the Gnutella peer-to-peer file sharing network from August 2002; each graph represents a different snapshot of the Gnutella network. Every host is denoted by a vertex and a connection from one host to another is denoted by an edge that points towards the latter. These networks were obtained from the Stanford Large Network Dataset Collection <https://snap.stanford.edu/data/>.
  - **Electronic Circuits [35, 50, 51]**. Network representations of electronic circuits from the ISCAS89 benchmark collection. Logic gates and flip-flops are represented by vertices, and the directed connections between them are denoted edges. These networks were obtained from Uri Alon's website <https://www.weizmann.ac.il/mcb/UriAlon/download/collection-complex-networks>.
  - **Texas power grid [52]**. Network representation of the Texas power grid. Substations, generators, and transformers are represented by vertices, and transmission lines between them are denoted by edges, with the edge directionality corresponding to the electric power flow. This network was obtained directly from Yang-Yu Liu.
  - **Slashdot [46]**. Friend/foe network of the technology-related news website Slashdot obtained in 2009. Users are denoted by vertices, and a user tagging another user as a friend/foe is denoted by an edge pointing towards the latter user. In this work we reverse the edges in this network so that they match the direction of influence in a dynamic model (i.e., if a user tags another user, the latter has an influence on the former). This network was obtained from the Stanford Large Network Dataset Collection <https://snap.stanford.edu/data/>.

- **Wikivote [53, 54]**. Who-votes-for-whom network of Wikipedia users for administrator elections. Users are denoted by vertices, and a user voting for another user is denoted by an edge pointing towards the latter user. In this work we reverse the edges of this network so that they match the direction of influence in a dynamic model (i.e., if a user votes for another user, the latter has an influence on the former). This network was obtained from the Stanford Large Network Dataset Collection <https://snap.stanford.edu/data/>.
- **College student and prison inmate trust networks [55–57]**. Social networks of positive sentiment of college students in a course about leadership and of inmates in prison. Each person is denoted by a vertex, and the expression of a positive sentiment of a person towards another person (based on a questionnaire) is denoted by an edge pointing towards the latter. In this work we reverse the edges of this network so that they match the direction of influence in a dynamic model (i.e., if a person has a positive sentiment towards another, the latter has an influence on the former). These networks were obtained from Uri Alon’s website <https://www.weizmann.ac.il/mcb/UriAlon/download/collection-complex-networks>.
- **Epinions [58]**. Who-trusts-whom online social network of Epinions.com, a general consumer review site. Users are denoted by vertices, and a user trusting another user is denoted by an edge pointing towards the latter. In this work we reverse the edges of this network so that they match the direction of influence in a dynamic model (i.e., if a user trusts another user, the latter has an influence on the opinion of the former). This network was obtained from the Stanford Large Network Dataset Collection <https://snap.stanford.edu/data/>.
- **arXiv’s High Energy Physics - Theory and High Energy Physics - Phenomenology citation networks [59, 60]**. Citations between preprints in the e-print repository arXiv for the High Energy Physics - Theory (hep-th) and High Energy Physics - Phenomenology (hep-ph) sections. The citations cover the period from January 1993 to April 2003. Each preprint in the network is denoted by a vertex; a preprint citing another preprint is denoted by a directed edge from the citing preprint to the cited preprint. In this work we reverse the edges of this network so that they match the direction of influence in a dynamic model (i.e., if a preprint is cited by another preprint, the latter had an influence on the former). This network was obtained from the Stanford Large Network Dataset Collection <https://snap.stanford.edu/data/>.
- **UC Irvine online social network [61]**. Network of messages among users in an online community for students at University of California, Irvine. Users are denoted by vertices, and a user messaging another user is denoted by an edge pointing towards the latter. This network was obtained from Tore Opsahl’s website <https://toreopsahl.com/datasets/>.
- **Cellphone communication network [62]**. Call network of a subset of anonymized cellphone users. Each user is denoted by a vertex, and a call or text message from one user to another is denoted by a directed edge from the sender to the receiver. This network was obtained directly from Yang-Yu Liu.
- **E-mail communication network [63]**. Network of e-mails sent among users in a university during a period of 83 days. Each user is denoted by a vertex, and an e-mail sent from one user to another during this period of time is denoted by an edge from the sender to the receiver. This network was obtained directly from Yang-Yu Liu.
- **Intra-organizational Freeman networks [64]**. Network of personal relationships among researchers working on social network analysis at the beginning and at the end of the study. Each researcher is denoted by a vertex, and a personal relationship from a researcher to another is denoted by a directed edge from the former to the latter. In this work we reverse the edges of this network so that they match the direction of influence in a dynamic model (i.e., if a researcher has a personal relationship with another, the latter has an influence on the former). This network was obtained from Tore Opsahl’s website <https://toreopsahl.com/datasets/>.
- **Intra-organizational consulting and manufacturing networks [65]**. Network describing the relationships between employees in a consulting company and in a research team from a manufacturing company. Each employee involved is denoted by a vertex, and the frequency/extent of information or advice an employee obtains from another (as measured by a questionnaire) is denoted by a weighted, directed edge among them that points from the questioned employee. We follow [23] and [22], and use all edges with a nonzero weight to define a unweighted network, which we use for our analysis. We also reverse the edges of this network so that they match the direction of influence in a dynamic model (i.e., if an employee receives advice or information from another, the latter has an influence on the former). This network was obtained from Tore Opsahl’s website <https://toreopsahl.com/datasets/>.

### III.B. Notes on the ensembles of randomized real networks

We study the control properties of ensembles of randomized real networks using four randomization procedures. We follow [23] and [22] in using full randomization, which turns the network into a directed Erdős-Rényi network with  $N$  nodes and  $M$  edges [66], and degree-preserving randomization, which keeps the in-degree and out-degree of every node but shuffles its successor and predecessor nodes [67]. Erdős-Rényi randomization is implemented by creating a graph of  $N$  nodes, randomly (uniformly) choosing a source and a target of an edge from the set of  $N$  nodes, and repeating this for each of the  $M$  edges. For the degree-preserving randomization, we start from the original network and choose two edges randomly (uniformly), for which we switch their target nodes if the target and source nodes of both edges are each different (if they are the same, we choose another edge pair). We repeat this step for a transient of  $25M$  times, after which we save the obtained network as the first element of the ensemble. We then repeat the target-node-switching step  $5M$  times, save the resulting network as the second element of the ensemble, and repeat the target-node-switching step  $5M$  times for each consequent ensemble element.

To verify that the cycle structure explains the observed FC node set size, we designed two new randomization procedures: an SCC-preserving and degree-preserving randomization in which the directed acyclic part of the graph is randomized and every edge that is part of an SCC is kept intact, and a short-cycle-preserving and degree-preserving randomization in which the randomized network is guaranteed to have every edge that is part of a short cycle in the original network.

For the SCC-preserving randomization, we first remove all edges that are part of an SCC, which leaves a network that is a directed acyclic graph (DAG, i.e., a graph with no cycles [68]). Starting from this DAG, we generate a topological order  $O = \{L(i)\}$  for each node  $i$  in the network in the following way<sup>7</sup>:

- 1.- Set  $order = 0$
- 2.- Set  $L$  to be the sink nodes in the DAG.
- 3.- Randomly (uniformly) select a node from  $L$  in the DAG, assign to it the value  $L(i) = L$ , and remove the selected node from the DAG.
- 4.- Repeat 2 and 3 with the updated DAG and increase the value  $order$  by 1 at after each repeat

<sup>7</sup> In a topological order, each node  $i$  is assigned a positive integer  $L(i)$  in such a way that for all pairs of nodes  $i, j$  if node  $i$  has an outgoing edge to node  $j$  then  $L(j) < L(i)$ . A topological order exists for a graph if and only if the graph is a DAG.

The result is a topological order  $O$ , which we use to generate the randomized network by following the same edge-rewiring procedure as in degree-preserving randomization but only accept an edge-rewiring step if it preserves the topological order  $O$ . We repeat the edge-rewiring step for a transient of  $25M$  times, after which we add back the edges in the SCCs and save the obtained network as an element of the ensemble. Each topological order  $O$  is chosen at random to make sure that the resulting network ensemble is not generated with a single topological order like some previous work on DAGs has [68]<sup>8</sup>

For the short-cycle-preserving randomization, we first remove all edges that are part of a cycle of length 4 or less, and follow the same edge-rewiring procedure as in degree-preserving randomization but only accept an edge-rewiring step if does not create a cycle of length 1 or 2. We repeat this step for a transient of  $25M$  times. We then do the same edge-rewiring step for a uniformly chosen edge on each cycle of length 4, a process which we repeat 10 times. This last step is repeated but for cycles of length 3. In the resulting network we add back the short-cycle edges of the original network, and save the resulting network as the first element of the ensemble. For every other element of the ensemble, we repeat the same procedure but use a transient of  $5M$  edge rewiring steps. For the short-cycle-preserving randomization of some networks, we omit the edge-rewiring step for cycles of length 4 (emails, political blogs, and UCI) or of length 3 and 4 (slashdot, wikivotes, nd.edu, Manufacturing, and epinions) because of the size and large number of cycles in these networks.

For each real network we used  $\Omega = 100$  networks as the ensemble size for the Erdős-Rényi (Fig. S2c) and degree-preserving randomizations, and  $\Omega = 50$  for the SCC-preserving and short-cycle-preserving randomizations. For most ensemble properties we used the 100 ensemble networks to estimate the average value and standard deviation of the property, but for some properties this was too computationally expensive for very large networks (e.g.  $FVS$  of networks with  $> 2.5 \times 10^4$  nodes) or for very dense networks (e.g. cycle numbers of intra-organizational networks). For these properties and networks, we used a smaller ensemble size, as specified below.

- Political blogs. For cycle numbers of length 4,  $\Omega = 10$ .
- nd.edu. For cycle numbers of length 4,  $\Omega = 2$ . For

<sup>8</sup> We note that the algorithm we use to generate a topological order samples from every possible topological order but does not sample them uniformly. One can show that the probability  $P$  of a topological order  $O$  is given by  $P(O) = 1/C(O)$ ,  $C(O) = l_1 \cdot l_2 \cdots l_N$ , where  $l_i$  is the number of elements in the list  $L$  at iteration  $i$  of the algorithm. Given that the objective of the algorithm is that the network ensemble is not generated with a single topological order, we consider this non-uniform sampling acceptable.

$N_{FVS}^{ER}$  and  $N_{FVS}^{Rand-deg}$ ,  $\Omega = 5$  and 1 iteration for GRASP. For  $N_{FVS}^{Rand-SCC}$  and  $N_{FVS}^{Rand-Cyc}$ ,  $\Omega = 50$  and 1 iteration for GRASP.

- stanford.edu. For cycle numbers of length  $\geq 2$ ,  $\Omega = 20$ . For  $N_{FVS}$ ,  $\Omega = 5$  and 1 iteration for GRASP. For the SCC-preserving and short-cycle-preserving randomization we omitted this network because of time and resource constraints.

- Slashdot. For cycle numbers of length  $\geq 3$ ,  $\Omega = 20$ . For  $N_{FVS}^{ER}$ ,  $N_{FVS}^{Rand-deg}$ ,  $N_{FVS}^{Rand-SCC}$ , and  $N_{FVS}^{Rand-Cyc}$ ,  $\Omega \geq 40$  and 2 iterations for GRASP.

- Epinions. For  $N_{FVS}^{ER}$ ,  $N_{FVS}^{Rand-deg}$ ,  $N_{FVS}^{Rand-SCC}$ , and  $N_{FVS}^{Rand-Cyc}$ ,  $\Omega = 50$  and  $\geq 2$  iterations for GRASP.

- arXiv HepTh, HepPh. For cycle numbers of length  $\geq 2$ ,  $\Omega = 50$ . For  $N_{FVS}^{ER/Rand-deg/Rand-SCC/Rand-Cyc}$ ,  $\Omega \geq 50$  and  $\geq 10$  iterations for GRASP.

- UCOnline. For cycle numbers of length 4,  $\Omega = 10$ .

- Cellphone. For  $N_{FVS}^{ER}$  and  $N_{FVS}^{Rand-deg}$ ,  $\Omega = 200$  and 50 iterations for GRASP. For  $N_{FVS}^{Rand-SCC}$  and  $N_{FVS}^{Rand-Cyc}$ ,  $\Omega = 50$  and 25 iterations for GRASP.

- Emails. For cycle numbers of length  $\geq 2$ ,  $\Omega = 5$ .

- Manufacturing. For cycle numbers of length  $\geq 2$ ,  $\Omega = 20$ .

### III.C. Comparing feedback vertex set control and structural controllability in real networks

SC was applied to diverse types of real networks and the ratio of the minimal number of SC nodes needed,  $N_{SC}$ , and the total number of nodes,  $n_{SC} = N_{SC}/N$  was used to gauge how difficult it is to control these networks [23]. Both SC and FC can be used to answer the question of which nodes need to be controlled in order to control a network (albeit they differ in the underlying dynamics they consider, their control objective, and their control actions), so a natural question is how the fraction of control nodes in real networks compares between SC and FC ( $n_{FC} = N_{FC}/N$ , where  $N_{FC}$  is the size of the minimal FC control set). To answer this question, we apply SC and FC to the real networks in [23], and compare the fraction of control nodes  $n_{SC}$  and  $n_{FC}$  (Fig. S7a and Table S1). A surprising result is that the fraction of control nodes  $n_{SC}$  and  $n_{FC}$  appears to be inversely related across several types of networks. For example, gene regulatory networks require between 75% - 96% of nodes in SC yet only require between 1% - 18% of nodes in FC. A similar  $n_{SC} \gg n_{FC}$  relationship is also seen in food web networks and internet networks, while the opposite relationship ( $n_{SC} \ll n_{FC}$ ) is seen in the social trust networks with low  $n_{SC}$  and intra-organizational networks.

To explain the topological properties underlying the difference in  $n_{SC}$  and  $n_{FC}$ , we note that the fraction of nodes  $n_{SC}$  and  $n_{FC}$  obey the relations

$$n_{SC} = n_s + n_e + n_i, \quad (\text{S11})$$

$$n_{FC} = n_s + n_{FVS}, \quad (\text{S12})$$

where  $n_s$  is the fraction of source nodes,  $n_e$  is the fraction of external dilations nodes in SC,  $n_i$  is the fraction of internal dilations nodes in SC, and  $n_{FVS}$  is the fraction of nodes in the FVS of the network. Empirical directed networks tend to have a bow-tie structure [66, 69], in which most of the network belongs to the largest strongly connected component (which contains most cycles in the network, and thus determines  $n_{FVS}$ ), its in-component (the nodes that can reach the strongly connected component, which thus determine  $n_s$ ), or its out-component (the nodes that can be reached from the strongly connected component, which thus determine  $n_e$ ). We define the fractions  $\eta_x = n_x/(n_s + n_e + n_i + n_{FVS})$ , where  $x = s, e, i, FVS$ . These fractions reflect the potential domination of a network component over the others. Eqs. S11-S12 and the bow-tie structure of real networks offer a topological explanation for the observed relationships between  $n_{SC}$  and  $n_{FC}$ .

Applying this reasoning to the studied real networks (Table S1), we find that all networks with  $n_{SC} < n_{FC}$  have a topology dominated by their SCC component ( $\eta_{FVS} \gg \eta_e, \eta_i, \eta_s$ , Fig. S7, brown shading; e.g. intra-organizational networks, the college students and prison inmates trust networks, and the *C. elegans* neural network). Most networks with  $n_{SC} > n_{FC}$  are dominated by their out-component ( $\eta_e \gg \eta_{FVS}, \eta_i, \eta_s$ , Fig. S7, yellow shading; e.g. gene regulatory networks, most food webs, and internet networks) or by internal dilations ( $\eta_i \gg \eta_{FVS}, \eta_e, \eta_s$ , Fig. S7, pink shading; e.g. metabolic networks and circuits). The rest of the networks have a mixed profile ( $\eta_{FVS} \simeq \eta_e \simeq \eta_i \simeq \eta_s$ , Fig. S7, no shading), and include networks with  $n_{SC} > n_{FC}$  (citation networks and the Texas power grid) and the networks in which  $n_{SC} \simeq n_{FC}$  (a political blog network and two online social communication networks).

## IV. Structure-based control of the *Drosophila melanogaster* segment polarity gene regulatory network

We compare the results of the two control methods for the gene regulatory network of the *Drosophila* segment polarity genes, for which several dynamic models exist [70–72]. The segment polarity genes, especially wingless (*wg*) and engrailed (*en*), are important determinants of embryonic pattern formation and contributors to embryonic development [70]. The wingless mRNA and protein are expressed in the cell that is anterior to the cell that expresses the engrailed and hedgehog (*hh*) mRNA and protein. All models consider a group of four subsequent cells as a repeating unit, and include intra-cellular and inter-cellular interactions.

The continuous model of von Dassow et al. represents each cell as a hexagon with six relevant cell-to-cell boundaries. It includes 136 nodes that represent mRNAs and proteins, among them 4 source nodes and 24 sink nodes, and 488 edges that represent transcriptional

regulation, translation, and protein-protein interactions. Fig. 4a in the main text, reproduced here as Fig. S3a, shows the network corresponding to the *wg*-expressing cell (cell 1) and three of its boundaries with the *en*-expressing cell 2. Additional nodes in the network include, *ptc* (patched), *ci* (cubitus interruptus), its proteins *CID* and *CN* (repressor fragment of *CID*), *IWG* (intracellular *WG* protein), *EWG* (extracellular *WG* protein), *PH* (complex of patched and hedgehog proteins), and *B*, a constitutive activator of *ci*. For each gene, the mRNA is written in lower case and the protein(s) are written in upper case. The nodes are characterized by continuous concentrations, whose rate of change is described by ordinary differential equations (ODE) involving Hill functions for gene regulation and mass action kinetics for protein-level processes, and using 48 kinetic parameters [73, 74]. von Dassow et al. have shown that the model can reproduce the essential feature of the wild type steady state: *wg/WG* are expressed anterior to the parasegment boundary (cell 1) and *en/EN/hh/HH* are expressed posterior to the parasegment boundary (cell 2) as shown in Fig. 4. The initial condition that yields this steady state for the most parameter sets, the so-called ‘‘ crisp’’ initial condition, *wg/IWG* in the first cell is at maximal concentration (1), *en/EN* in the second cell has concentration 1, the source nodes *B* are fixed at 0.4 in each cell and all the other nodes have zero concentration.

Wild type steady state of the von Dassow et al. model for the second parameter set provided by the *Ingeneue* program [73, 75], using normalized concentration variables

$$\begin{aligned}
c(en_2) &= c(EN_2) = 0.986, \\
c(wg_1) &= 0.857, \\
c(IWG_1) &= 0.006, \\
c(EWG_{0,0}) &= c(EWG_{0,3-5}) = 0.005, \\
c(EWG_{0,1}) &= c(EWG_{0,2}) = 0.011, \\
c(EWG_{1,0}) &= c(EWG_{1,3}) = 0.269, \\
c(EWG_{1,1-2}) &= c(EWG_{1,4-5}) = 0.264, \\
c(EWG_{2,0-3}) &= 0.005, \\
c(EWG_{2,4}) &= c(EWG_{2,5}) = 0.011, \\
c(ptc_0) &= c(ptc_1) = c(ptc_3) = 0.995, \\
c(ptc_2) &= 0.001, \\
c(PTC_{0,*}) &= c(PTC_{1,*}) = c(PTC_{3,*}) = 0.166, \\
c(ci_0) &= c(ci_1) = c(ci_3) = 0.868, \\
c(ci_2) &= 0.007, \\
c(CI_0) &= c(CI_1) = c(CI_3) = 0.057, \\
c(CI_2) &= 0.005, \\
c(CN_0) &= c(CN_1) = c(CN_3) = 0.42, \\
c(CN_2) &= 0.001, \\
c(hh_2) &= 1, \\
c(HH_{2,0}) &= c(HH_{2,3}) = 0.072, \\
c(PH_{1,1-2}) &= c(PH_{3,4-5}) = 0.001,
\end{aligned}$$

where  $i, *$  represents all sides of the  $i$ th cell. The concentration of the other nodes is smaller than  $10^{-5}$ .

Another initial condition considered here is a nearly-null initial condition, wherein intra-cellular nodes have a concentration of 0.05 in the first and third cell and 0.15 in the second and fourth (zeroth) cell; membrane-localized nodes have concentration of 0.15 for even-numbered sides and 0.05 for odd-numbered sides in every cell. This initial condition yields an unpatterned steady state for the majority of parameter sets.

Unpatterned steady state of the von Dassow et al. model, for the second parameter set provided by the *Ingeneue* program [73, 75], using normalized concentrations:

$$\begin{aligned}
c(wg_*) &= 0.857, \\
c(IWG_*) &= 0.007 \\
c(EWG_{*,*}) &= 0.28, \\
c(ptc_*) &= 0.996, \\
c(PTC_{*,*}) &= 0.166, \\
c(ci_*) &= 0.868, \\
c(CI_*) &= 0.057, \\
c(CN_*) &= 0.42,
\end{aligned}$$

where  $*$  represents for all cells, and  $*, *$  represents for all sides in all cells. The concentration of the other nodes is smaller than  $10^{-5}$ .

The differential equation system is solved using a custom code in Python and the `odeint` function with default parameter setting. We used the differential equations given in the appendix of [74]. *Ingeneue* can be found at <http://rusty.fhl.washington.edu/ingeneue/papers/papers.html>.

The Boolean model implements a few modifications in the network topology compared with the ODE network model, and considers only two cell-to-cell boundaries instead of six. There are 56 nodes and 144 edges in the network as shown in Fig. 4b. One difference compared with the von Dassow et al. model is the existence of three cubitus interruptus proteins: the main protein *CI*, and two derivatives with opposite function: *CIA*, which is a transcriptional activator, and *CIR*, a transcriptional repressor. There are four source nodes, representing the sloppy paired protein (*SLP*), which is known to have a sustained expression in two adjacent cells (cells 0 and 1 if the *wg*-expressing cell is considered cell 1) and is absent from the other two. There are ten steady states for this Boolean network model when considering the biologically relevant pattern of the source node states. Starting from the biologically known wild type initial condition, which consists of the expression (ON state) of *SLP*<sub>0</sub>, *SLP*<sub>1</sub>, *wg*<sub>1</sub>, *en*<sub>2</sub>, *hh*<sub>2</sub>, *ci*<sub>0</sub>, *ci*<sub>1</sub>, *ci*<sub>3</sub>, *ptc*<sub>0</sub>, *ptc*<sub>1</sub>, *ptc*<sub>3</sub>, the model converges into the biologically known wild type steady state illustrated on Fig. 4c.

Specifically, the wild type steady state of the Albert &

Othmer model consists of the expression of

$$SLP_0, SLP_1, wg_1, WG_1, en_2, EN_2, hh_2, HH_2, \\ ci_0, ci_1, ci_3, CI_0, CI_1, CI_3, CIA_1, CIA_3, CIR_0, \\ ptc_1, ptc_3, PTC_0, PTC_1, PTC_3, PH_1, PH_3.$$

Analytical solution reported in [74] indicated that the states of the  $wg$  and  $PTC$  nodes, each of which has a positive auto-regulatory loop, determine the steady state for the given source node ( $SLP$ ) configuration [71]. For example, any initial condition with no  $wg$  expression leads to an unpatterned steady state wherein  $ptc$ ,  $ci$ ,  $CI$  and  $CIR$  are expressed in each cell, and the rest of the nodes are not expressed in any cell.

#### IV.A. Structure-based control of the von Dassow et al. differential equation model

The FC method predicts that one needs to control  $N_{FC} = 52$  nodes (4 source nodes and 48 additional nodes) to lead any initial condition to converge to any original attractor of the model. There are multiple control sets with  $N_{FC} = 52$ ; one of them consists of  $B$  (source node),  $CI$ ,  $CN$ ,  $IWG$ ,  $EWG$  on every other side,  $HH$  on every other side,  $PTC$  on every other side in all four cells (shown in Fig. S3a). We perform simulations using two benchmark parameter sets to test this prediction. We use the second parameter set provided by the Ingenu program to test the system's convergence to a steady state [73, 75]. The ODE system has at least two steady states with this parameter set. A nearly null initial condition leads to the unpatterned state (illustrated by the green lines in Fig. 4d in the main text). The crisp initial condition leads to the wild type pattern (see pink lines in Fig. 4d), which we choose as the desired steady state. If we start from the nearly null initial condition and maintain the concentrations of the nodes in the FC node set in the values they would have in the desired steady state, the system evolves into the desired steady state (see blue lines and inset of Fig. 4d). We obtained the same success of FC control when starting from 100 different random initial conditions (shown in Fig. S4a). We also obtained the same success using a reduced FC set (blue lines in Fig. S4b), which consists of  $B$ ,  $CID$ ,  $CN$ ,  $IWG$  in every cell. In contrast, in the absence of control none of the trajectories converge to the wild type steady state (red lines in Fig. S4b).

We also numerically verified, using a different benchmark parameter set, namely the first parameter set provided by the Ingenu program, that FC control can also successfully drive any state to a limit cycle attractor (see Fig. S8a). This limit cycle attractor has the same expression pattern of  $en$ ,  $wg$  and  $hh$  as the wild type steady state, thus we refer to it as the wild type limit cycle (illustrated in Fig. S8c). We also obtained the same success of driving any state to a limit cycle attractor using the same reduced Feedback vertex control shown in Fig. S8b.

SC control indicates multiple control sets with  $N_{SC} = 24$  nodes. One possible combination is  $B_*$ ,  $PTC_{*,1}$ ,  $PTC_{*,3}$ ,  $PTC_{*,5}$ ,  $HH_{*,5}$ ,  $PH_{*,1}$ , where  $*$  represents all cells (shown in Fig. S3b). Though SC predicts that less nodes need to be controlled, applying it requires a potentially complicated time-varying driver signal, which would need to be determined for each initial condition using, for example, minimum-energy control or optimal control [15, 76].

#### IV.B. Structure-based control of the Albert & Othmer Boolean model

The FC method predicts that  $N_{FC} = 14$  nodes need to be controlled, including the 4 source nodes ( $SLP$ ), the 8 self-sustaining nodes (all  $wg$  and  $PTC$ ), and 2 additional nodes (with one possibility being  $CIR_1$  and  $CIR_3$ ). Since the FC set contains all  $wg$  and  $PTC$  nodes, which were shown to determine the steady states under the indicated source node states, we can conclude that controlling the nodes in the FC set is enough to drive any initial condition to the desired steady state in the Albert & Othmer model. The simulation result is consistent with the theoretical result, as shown in Fig. 4e. The wild type initial condition leads to the wild type steady state (pink lines). The null initial condition used in the Boolean model is that all the nodes are in the OFF state; the resulting steady state is the unpatterned steady state (green lines). The controlled trajectory with FC is shown in blue lines. We obtained the same success of FC control when starting from 100 different random initial conditions, as shown in Fig. S5a. Moreover, the 12 nodes consisting of  $SLP$ ,  $wg$  and  $PTC$  in each cell (which we refer to as the reduced FC set) are enough to drive all the random initial conditions to the desired steady state in this particular model, as shown in Fig. S5b.

SC control predicts that we only need to control the four source nodes ( $SLP$ ), as the network can be covered by four branches and one loop. Relevant to this, Albert & Othmer studied three scenarios of fixed states of the source nodes. If the source nodes are locked into their respective states in the wild type steady state (two ON and two OFF), there are six reachable attractors, one of which is the wild type steady state. If all source nodes are locked into the OFF state, there are seven attractors, but none of them is the wild type steady state. If all source nodes are locked into the ON state, the unpatterned state is the only attractor. These results suggest that the correct expression of the source nodes is necessary, but not sufficient for attractor control of the system. Indeed, SC can make no such guarantee, since for general nonlinear systems it only provides sufficient conditions for local controllability around a steady state or a system trajectory.

For a simplified, single-cell version of the Albert & Othmer model, Gates and Rocha showed that the SC node set is sufficient for attractor control, but does not fully

control this system [31]. Thus, a control method such as

[77, 78] seems to be required for correctly predicting full control node sets in Boolean models.

- 
- [1] Fiedler B, Mochizuki A, Kurosawa G, Saito D (2013). Dynamics and control at feedback vertex sets. I: Informative and determining nodes in regulatory networks. *Journal of Dynamics and Differential Equations* 25(3), 563-604.
- [2] Mochizuki A, Fiedler B, Kurosawa G, Saito D (2013). Dynamics and control at feedback vertex sets. II: A faithful monitor to determine the diversity of molecular activities in regulatory networks. *J Theor Biol.* 335, 130-146.
- [3] Tyson JJ, Chen KC, Novak B (2003). Sniffers, buzzers, toggles and blinkers: dynamics of regulatory and signaling pathways in the cell. *Curr Opin Cell Biol.* 15(2), 221-231.
- [4] Bassett DS, Alderson DL, Carlson JM (2012). Collective decision dynamics in the presence of external drivers. *Phys Rev E* 86 (3), 036105.
- [5] Festa, P., Pardalos, P. M., & Resende, M. G. (1999). Feedback set problems. In *Handbook of combinatorial optimization* (pp. 209-258). Springer US.
- [6] Karp, R. M. (1972). Reducibility among combinatorial problems. RE Miller, JW Thatcher (Eds.), *Complexity Of Computer Computations*, Plenum Press, New York, 85-103.
- [7] Even, G., Naor, J. S., Schieber, B., & Sudan, M. (1998). Approximating minimum feedback sets and multicuts in directed graphs. *Algorithmica*, 20(2), 151-174.
- [8] Resende, M. G. (2009). Greedy randomized adaptive search procedures greedy randomized adaptive search procedures. *Encyclopedia of optimization*, 1460-1469.
- [9] Pardalos, P. M., Qian, T., & Resende, M. G. (1998). A greedy randomized adaptive search procedure for the feedback vertex set problem. *Journal of Combinatorial Optimization*, 2(4), 399-412.
- [10] Festa, P., Pardalos, P. M., & Resende, M. G. (2001). Algorithm 815: FORTRAN subroutines for computing approximate solutions of feedback set problems using GRASP. *ACM Transactions on Mathematical Software (TOMS)*, 27(4), 456-464.
- [11] Galinier, P., Lemamou, E., & Bouzidi, M. W. (2013). Applying local search to the feedback vertex set problem. *Journal of Heuristics*, 19(5), 797-818.
- [12] Zañudo JGT, Albert R (2015). Cell fate reprogramming by control of intracellular network dynamics. *PLoS Comput Biol.* 11(4), e1004193.
- [13] Remy, É., Ruet, P., & Thieffry, D. (2008). Graphic requirements for multi-stability and attractive cycles in a Boolean dynamical framework. *Advances in Applied Mathematics*, 41(3), 335-350
- [14] Slotine JJE, Li W (1991). *Applied nonlinear control* (Vol. 199, No. 1). Prentice-Hall.
- [15] Liu YY, Barabási AL (2016). Control principles of complex systems. *Rev Mod Phys.* 88(3), 035006.
- [16] Isidori, A. (2013). *Nonlinear control systems*. Springer Science & Business Media.
- [17] Cornelius SP, Kath WL, Motter AE (2013). Realistic control of network dynamics. *Nat Commun.* 4, 1942.
- [18] Wang LZ et al. (2016). A geometrical approach to control and controllability of nonlinear dynamical networks. *Nat Commun.* 7, 11323.
- [19] Kalman, R. E. (1963). Mathematical description of linear dynamical systems. *Journal of the Society for Industrial and Applied Mathematics, Series A: Control*, 1(2), 152-192.
- [20] Lin CT (1974). Structural controllability. *IEEE Trans Automat Contr.* 19(3), 201-208.
- [21] Shields RW, Pearson JB (1975). Structural controllability of multi-input linear systems. *IEEE Trans Automat Contr.* 21, 203-212.
- [22] Ruths J, Ruths D (2014). Control profiles of complex networks. *Science* 343(6177), 1373.
- [23] Liu YY, Slotine JJ, Barabási AL (2011). Controllability of complex networks. *Nature* 473(7346), 167-173.
- [24] Cowan, N. J., Chastain, E. J., Vilhena, D. A., Freudenberg, J. S., & Bergstrom, C. T. (2012). Nodal dynamics, not degree distributions, determine the structural controllability of complex networks. *PloS one*, 7(6), e38398.
- [25] Sun, J. & Motter, A. E. (2013). Controllability transition and nonlocality in network control. *Physical review letters*, 110(20), 208701.
- [26] Zhao, C., Wang, W. X., Liu, Y. Y., & Slotine, J. J. (2015). Intrinsic dynamics induce global symmetry in network controllability. *Scientific reports*, 5.
- [27] Chen, Y. Z., Wang, L. Z., Wang, W. X., & Lai, Y. C. (2016). Energy scaling and reduction in controlling complex networks. *Royal Society open science*, 3(4), 160064.
- [28] Vinayagam A et al. (2015). Controllability analysis of the directed human protein interaction network identifies disease genes and drug targets. *Proc Natl Acad Sci USA* 113(18) 4976.
- [29] Kawakami E et al. (2016). Network analyses based on comprehensive molecular interaction maps reveal robust control structures in yeast stress response pathways. *NPJ Syst Biol Appl.* 2, 15018.
- [30] Gu S et al. (2015). Controllability of structural brain networks. *Nat Commun.* 6, 8414.
- [31] Gates AJ, Rocha LM (2015). Control of complex networks requires both structure and dynamics. *Sci Rep.* 6 (24456).
- [32] Gama-Castro, S., Jiménez-Jacinto, V., Peralta-Gil, M., Santos-Zavaleta, A., Peñaloza-Spinola, M. I., Contreras-Moreira, B., ... & Bonavides-Martínez, C. (2008). RegulonDB (version 6.0): gene regulation model of *Escherichia coli* K-12 beyond transcription, active (experimental) annotated promoters and Textpresso navigation. *Nucleic acids research*, 36(suppl 1), D120-D124.
- [33] Shen-Orr, S. S., Milo, R., Mangan, S., & Alon, U. (2002). Network motifs in the transcriptional regulation network of *Escherichia coli*. *Nature genetics*, 31(1), 64-68.
- [34] Balaji, S., Babu, M. M., Iyer, L. M., Luscombe, N. M., & Aravind, L. (2006). Comprehensive analysis of combinatorial regulation using the transcriptional regulatory network of yeast. *Journal of molecular biology*, 360(1), 213-227.
- [35] Milo, R., Shen-Orr, S., Itzkovitz, S., Kashtan, N.,

- Chklovskii, D., & Alon, U. (2002). Network motifs: simple building blocks of complex networks. *Science*, 298(5594), 824-827.
- [36] Norlen, K., Lucas, G., Gebbie, M., & Chuang, J. (2002, August). EVA: Extraction, visualization and analysis of the telecommunications and media ownership network. In Proceedings of International Telecommunications Society 14th Biennial Conference (ITS2002), Seoul Korea.
- [37] Jeong, H., Tombor, B., Albert, R., Oltvai, Z. N., & Barabási, A. L. (2000). The large-scale organization of metabolic networks. *Nature*, 407(6804), 651-654.
- [38] Watts, D. J., & Strogatz, S. H. (1998). Collective dynamics of 'small-world' networks. *nature*, 393(6684), 440-442.
- [39] White, J. G., Southgate, E., Thomson, J. N., & Brenner, S. (1986). The structure of the nervous system of the nematode *Caenorhabditis elegans*: the mind of a worm. *Phil. Trans. R. Soc. Lond.*, 314, 1-340.
- [40] Huxham, M., Beaney, S., & Raffaelli, D. (1996). Do parasites reduce the chances of triangulation in a real food web? *Oikos*, 284-300.
- [41] Dunne, J. A., Williams, R. J., & Martinez, N. D. (2002). Food-web structure and network theory: the role of connectance and size. *Proceedings of the National Academy of Sciences*, 99(20), 12917-12922.
- [42] Christian, R. R., & Luczkovich, J. J. (1999). Organizing and understanding a winter's seagrass foodweb network through effective trophic levels. *Ecological Modelling*, 117(1), 99-124.
- [43] Martinez, N. D., Hawkins, B. A., Dawah, H. A., & Feifarek, B. P. (1999). Effects of sampling effort on characterization of food-web structure. *Ecology*, 80(3), 1044-1055.
- [44] Martinez, N. D. (1991). Artifacts or attributes? Effects of resolution on the Little Rock Lake food web. *Ecological Monographs*, 61(4), 367-392.
- [45] Adamic, L. A., & Glance, N. (2005, August). The political blogosphere and the 2004 US election: divided they blog. In Proceedings of the 3rd international workshop on Link discovery (pp. 36-43). ACM.
- [46] Leskovec, J., Lang, K. J., Dasgupta, A., & Mahoney, M. W. (2009). Community structure in large networks: Natural cluster sizes and the absence of large well-defined clusters. *Internet Mathematics*, 6(1), 29-123.
- [47] Albert, R., Jeong, H., & Barabási, A. L. (1999). Internet: Diameter of the world-wide web. *Nature*, 401(6749), 130-131.
- [48] Matei, R., Iamnitchi, A., & Foster, I. (2002). Mapping the Gnutella network. *Internet Computing, IEEE*, 6(1), 50-57.
- [49] Leskovec, J., Kleinberg, J., & Faloutsos, C. (2007). Graph evolution: Densification and shrinking diameters. *ACM Transactions on Knowledge Discovery from Data (TKDD)*, 1(1), 2.
- [50] Brglez, F., Bryan, D., & Kozminski, K. (1989, May). Combinational profiles of sequential benchmark circuits. In *Circuits and Systems, 1989., IEEE International Symposium on* (pp. 1929-1934). IEEE.
- [51] i Cancho, R. F., Janssen, C., & Solé, R. V. (2001). Topology of technology graphs: Small world patterns in electronic circuits. *Physical Review E*, 64(4), 046119.
- [52] Bianconi, G., Gulbahce, N., & Motter, A. E. (2008). Local structure of directed networks. *Physical review letters*, 100(11), 118701.
- [53] Leskovec, J., Huttenlocher, D., & Kleinberg, J. (2010, April). Signed networks in social media. In Proceedings of the SIGCHI conference on human factors in computing systems (pp. 1361-1370). ACM.
- [54] Leskovec, J., Huttenlocher, D., & Kleinberg, J. (2010, April). Predicting positive and negative links in online social networks. In Proceedings of the 19th international conference on World wide web (pp. 641-650). ACM.
- [55] Milo, R., Itzkovitz, S., Kashtan, N., Levitt, R., Shen-Orr, S., Ayzenshtat, I., ... & Alon, U. (2004). Superfamilies of evolved and designed networks. *Science*, 303(5663), 1538-1542.
- [56] Zeleny, L. D. (1950). Adaptation of research findings in social leadership to college classroom procedures. *Sociometry*, 13(4), 314-328.
- [57] MacRae, D. (1960). Direct factor analysis of sociometric data. *Sociometry*, 23(4), 360-371.
- [58] Richardson, M., Agrawal, R., & Domingos, P. (2003). Trust management for the semantic web. In *The Semantic Web-ISWC 2003* (pp. 351-368). Springer Berlin Heidelberg.
- [59] Leskovec, J., Kleinberg, J., & Faloutsos, C. (2005, August). Graphs over time: densification laws, shrinking diameters and possible explanations. In Proceedings of the eleventh ACM SIGKDD international conference on Knowledge discovery in data mining (pp. 177-187). ACM.
- [60] Gehrke, J., Ginsparg, P., & Kleinberg, J. (2003). Overview of the 2003 KDD Cup. *ACM SIGKDD Explorations Newsletter*, 5(2), 149-151.
- [61] Opsahl, T., & Panzarasa, P. (2009). Clustering in weighted networks. *Social networks*, 31(2), 155-163. Chicago
- [62] Song, C., Qu, Z., Blumm, N., & Barabási, A. L. (2010). Limits of predictability in human mobility. *Science*, 327(5968), 1018-1021.
- [63] Eckmann, J. P., Moses, E., & Sergi, D. (2004). Entropy of dialogues creates coherent structures in e-mail traffic. *Proceedings of the National Academy of Sciences of the United States of America*, 101(40), 14333-14337.
- [64] Freeman, S. C., & Freeman, L. C. (1979). The networkers network: A study of the impact of a new communications medium on sociometric structure. School of Social Sciences University of Calif..
- [65] Cross, R. L., & Parker, A. (2004). The hidden power of social networks: Understanding how work really gets done in organizations. Harvard Business Review Press.
- [66] Newman, M. (2010). *Networks: an introduction*. OUP Oxford.
- [67] Maslov S, Sneppen K (2002). Specificity and stability in topology of protein networks. *Science* 296(5569), 910-913.
- [68] Karrer B, Newman ME (2009). Random acyclic networks. *Phys Rev Lett*. 102(12), 128701.
- [69] Broder, A., Kumar, R., Maghoul, F., Raghavan, P., Rajagopalan, S., Stata, R., ... & Wiener, J. (2000). Graph structure in the web. *Computer networks*, 33(1), 309-320.
- [70] Von Dassow G, Meir E, Munro EM, Odell GM (2000). The segment polarity network is a robust developmental module. *Nature*, 406(6792), 188-192.
- [71] Albert R, Othmer HG (2003). The topology of the regulatory interactions predicts the expression pattern of the segment polarity genes in *Drosophila melanogaster*. *J Theor Biol*. 223,1.
- [72] Chaves, M., Sontag, E. D., & Albert, R. (2006). Methods of robustness analysis for Boolean models of gene control networks. *IEE Proc.-Syst. Biol*, 153(4), 154.

- [73] Von Dassow, G., & Odell, G. M. (2002). Design and constraints of the *Drosophila* segment polarity module: robust spatial patterning emerges from intertwined cell state switches. *Journal of Experimental Zoology*, 294(3), 179-215.
- [74] Daniels, B. C., Chen, Y. J., Sethna, J. P., Gutenkunst, R. N., & Myers, C. R. (2008). Sloppiness, robustness, and evolvability in systems biology. *Current opinion in biotechnology*, 19(4), 389-395.
- [75] Meir, E., Munro, E. M., Odell, G. M., & Von Dassow, G. (2002). Ingeneue: a versatile tool for reconstituting genetic networks, with examples from the segment polarity network. *Journal of Experimental Zoology*, 294(3), 216-251.
- [76] Kirk, D. E. (2012). *Optimal control theory: an introduction*. Dover Publications.
- [77] Akutsu, T., Hayashida, M., Ching, W. K., & Ng, M. K. (2007). Control of Boolean networks: hardness results and algorithms for tree structured networks. *Journal of Theoretical Biology*, 244(4), 670-679.
- [78] Cheng, D., & Qi, H. (2009). Controllability and observability of Boolean control networks. *Automatica*, 45(7), 1659-1667.